cannot out compete [^{3}H]9cRA at all. This difference in the ability of TChTOH to compete with [^{3}H]9cRA and [^{14}C]TPTOH may be caused by differences in their ligand-protein contacts (see following paragraph). These results suggest that the affinity of tin compounds to RXR is related to both the numbers and lengths of their alkyl groups.

RXR has been characterized as a nuclear receptor that demonstrates a highly restricted substrate specificity. Until recently, 9cRA was defined as the most potent RXR activator. However, various fatty acids, such as docosahexaenoic acid (DHA) and phytanic acid, and methoprene acid, a synthetic juvenile hormone analog used as an insect regulator, have been identified as RXR ligands (58–62). In addition, several retinoids with RXR selectivity have been developed (63), because retinoids are important therapeutic agents in the treatment of cancer and proliferative diseases of the skin. Although fatty acid- or methoprene acid-induced RXR activation requires greater than 1000-fold higher concentrations than that induced by 9cRA (58–62), the protein-ligand interactions of almost all RXR ligands share several common characteristics. Recently, Egea *et al.* (64) have obtained some interesting findings through analyzing the crystal structures of RXR with DHA, the synthetic ligand BMS649, and 9cRA. For example, RXR ligands contain a carboxylate group, which is important in their ability to be buried stably in the predominantly hydrophobic pocket. This functional group is involved in an ionic interaction with the strictly conserved basic residue R316 of helix H5 and forms a hydrogen bond with the backbone carbonyl amide group of the β-turn residue A327. Furthermore, ligand atoms C14–C22 of DHA and the tetrahydrotetramethylnaptho group of BMS649 occupy the same hydrophobic cavity (delineated by helices H3, H7, and H11), in which the β-ionone ring of 9cRA is buried stably. However, although trialkyltin compounds bind RXR with high specificity and induce RXR activation at doses similar to those of 9cRA, they lack a carboxylate group. Further, except for the TPT derivatives and TChTOH, RXR-stimulating trialkyltin compounds also lack sufficiently long fatty acid and cyclic functional groups, both of which might be buried in the β-ionone binding subpocket. In the competitive ligand-binding assay, RXR-stimulating trialkyltin compounds, except for TChTOH, completely out competed both [^{3}H]9cRA and [^{14}C]TPTOH, whereas 9cRA could not completely out-compete [^{14}C]TPTOH for binding to RXR. In addition, TChTOH out competed [^{14}C]TPTOH but not [^{3}H]9cRA. Together, these results suggest that the protein-ligand interaction of trialkyltin compounds and RXR is very different from those seen with other RXR ligands. Indeed, previous studies have reported that, despite the overall similarity of protein-ligand interactions, RXR ligands differ, especially within the L-shaped binding pocket. Although further studies are necessary to clarify which amino acid of RXR is important to the binding of trialkyltin compounds to the ligand-binding pocket, the ligand-protein contacts of these trialkyltin compounds are probably unique to them.

To our knowledge, ours is the first study to clarify the molecular mechanism of trialkyltin-induced endocrine-disrupting effects in the human placenta. Through RXR activation, trialkyltin compounds may be potent endocrine disruptors of other human tissues, because these compounds alter the endocrine functions, differentiation, and other processes of several human cell types (21, 47, 65–67). Furthermore, we demonstrated that trialkyltin compounds function as RXR ligands with novel structures, which bind to the LBD of RXR with high affinity and stimulate transcription of the receptor. We believe that our results provide information useful in the design of novel RXR ligands.

MATERIALS AND METHODS

Chemicals and Cell Culture

TBTCl, TPTOH, TOTH, and $DBTCl_2$ were obtained from Tokyo Kasei Kougyo (Tokyo, Japan). $SnCl_4$, TMTCl, TETBr, TChTOH, $MBTCl_3$, $MPTCl_3$, $DPTCl_2$, TPTCl, TBTH, TBTBr, TeBT, and TBVT were obtained from Aldrich Chemicals (Milwaukee, WI). 9cRA, atRA, AM580, and CDCA were obtained from Sigma Chemical Co. (St. Louis, MO). $15dPGJ_2$ and rosiglitazone were obtained from Cayman Chemical (Ann Arbor, MI). TPrTCl was obtained from Merck (Darmstadt, Germany). LG100268 (>95% pure) was synthesized in the Medical Chemistry Laboratories of Fujisawa Pharmaceutical (Osaka, Japan). Human choriocarcinoma cell lines Jar and JEG-3 were obtained from American Type Culture Collection (ATCC; Manassas, VA). Jar cells (ATCC No. HTB-144) were cultured in RPMI 1640 medium with 2 mM L-glutamine, 1 mM pyruvate, 4.5 g/liter glucose, and 10% fetal calf serum (FCS). JEG-3 cells (ATCC no. HTB-36) were cultured in MEM with 2 mM L-glutamine, 0.1 mM MEM nonessential amino acid solution (Invitrogen, Carlsbad, CA), and 10% FCS. To determine the effect of tin compounds on hCG secretion, aromatase activity, and mRNA expression of Jar cells, the cells were seeded and precultured for 24 h and then treated with either various concentrations of tin compounds in 0.1% dimethyl sulfoxide (DMSO) or vehicle alone (0.1% DMSO) for an additional 24 or 48 h. In control experiments, 0.1% DMSO did not alter hCG secretion, aromatase activity, mRNA expression of hCGβ and aromatase, or the results of reporter gene assays in any of the cell lines examined.

Determination of hCG Production in Culture Media

hCG production was assessed as previously described (27). Jar cells were seeded in 48-well plates (4×10^4 cells per well) in regular culture medium supplemented with 5% charcoal-stripped FCS instead of 10% normal FCS. After 24 h, cells were treated with various tin compounds for 48 h. To determine hCG production, the cells were then washed and cultured in fresh medium for another 24 h. Culture supernatant was collected, and hCG concentration was determined by ELISA. Microtiter ELISA plates were coated with 5 μg/ml rabbit polyclonal antibody against intact hCG in 0.05 M sodium bicarbonate, 0.02 M sodium carbonate buffer (pH 9.6) overnight at 4 C. They were blocked for 2 h at room temperature with 1% (wt/vol) gelatin in PBS, washed with 0.05% (vol/vol) Tween 20 in PBS (TPBS), and incubated for 2 h at 37 C with 50 μl collected test samples. After being washed three times with TPBS, the plates then were incubated for 2 h at 37

C with 1:1000 mouse monoclonal antibody against the β-subunit of hCG. After being washed with TPBS, the plates were incubated for an additional 2 h at 37 C with 1:1000 rabbit antimouse IgG1 antibody conjugated with horseradish peroxidase (Zymed Laboratories, Inc., South San Francisco, CA). The plates then were washed with TPBS and developed using 2.5 mM 2,2′-azinobis(3-ethylbenzothiazoline-6-sulfonic acid) diammonium salt (Sigma) in 0.1 M citrate buffered solution containing 0.015% H_2O_2. The reaction was stopped by the addition of 0.1% NaN_3, after which the plates were read at a wavelength of 415 nm in a microplate reader (Bio-Rad Laboratories, Inc., Hercules, CA). The level of hCG in the culture supernatant was calculated from a standard curve by using Microplate Manager III software (Bio-Rad). The standardized hCG was a kind gift from Teikoku Hormone Manufacturing (Tokyo, Japan).

Aromatase Assay

Aromatase activity was determined as previously described (27). Jar cells were seeded in 12-well plates (1.5×10^5 cells per well) in regular culture medium supplemented with 5% charcoal-stripped FCS instead of 10% normal FCS. After 24 h, cells were treated with various tin compounds for 48 h. At the end of each treatment, cells were washed three times with PBS. Aromatase activity then was determined by tritium release assay. This method measures production of ^3H_2O, which forms as a result of aromatization of the substrate [1β-^{3}H]androst-4-ene-3,17-dione (New England Nuclear, Boston, MA). Serum-free medium containing [1β-^{3}H]androst-4-ene-3,17-dione solution (54 nM) was prepared, and 0.5 ml of this solution was added to each well. In addition, wells containing media alone were tested to provide control values for aromatase activity. After incubation for 1 h, each plate was placed on ice, and 200 μl of culture medium was withdrawn from each well. The medium was extracted with 500 μl chloroform, vortexed, and then centrifuged for 1 min at 9000 × *g*. A 100-μl aliquot of the aqueous phase was mixed with 100 μl of a 5% wt/vol charcoal 0.5% wt/vol dextran T-70 suspension, vortexed, and then incubated for 10 min. After centrifugation of the solution for 5 min at 9000 × *g*, a 150-μl aliquot was removed to measure the level of radioactivity by liquid scintillation.

Quantitative RT-PCR

Jar cells were seeded in 100-mm tissue culture plates (1×10^6 cells) and treated with various compounds in regular culture medium supplemented with 5% charcoal-stripped FCS instead of 10% normal FCS, after which total RNA was extracted from them using TRIzol reagent (Invitrogen). mRNA expression of hCGβ and aromatase in Jar cells was determined by quantitative RT-PCR, as previously described (27). Total RNA (5 μg) extracted from Jar cells was reverse transcribed using SuperScript II reagent (Invitrogen) and oligo-(dT) as primer. The reaction was performed by incubation for 1 h at 42 C. After termination of cDNA synthesis, reaction mixtures were diluted with 4 volumes of Tris-EDTA. Aliquots (2 μl) of diluted reverse transcribed products were amplified in a reaction mixture containing 2× buffer from the QuantiTect SYBR Green PCR kit (QIAGEN, Valencia, CA) and 0.5 μM of each primer by using LightCycler (Roche Diagnostics, Mannheim, Germany). After preincubation at 95 C for 15 min, PCR was performed with 35–40 cycles of denaturation at 95 C for 15 sec, annealing at 65 C for 30 sec, and elongation at 72 C for 10 sec. Primers used were as follows: human aromatase, 5′-CCGGCCTTGTTCGTATGGTCA-3′ and 5′-CAACACGTCCACATAGCCCGA-3′; hCGβ, 5′-CCGTGTGCATCACCGTCAACA-3′ and 5′-GTTGCACACCACCTGAGGCAG-3′; and human β-actin, 5′-CTACGAGCTGCCTGACGGC-3′ and 5′-GCCACAGGACTCCATGCCC-3′.

Plasmid Construction

Human RXRα and RARβ cDNAs were amplified by RT-PCR using total RNA from JEG-3 cells. The amplified RXRα fragment was cloned into pSVSPORT1 (Invitrogen), whereas the RARβ fragment was cloned into a simian virus 40 promotor-containing expression vector. The resulting RXRα and RARβ expression vectors were termed pSVhRXRα and pSV40hRARβ, respectively. A 2.4-kb promoter I.1 sequence of the human aromatase gene (−2295 to +107 bp) was PCR amplified from JEG-3 genomic DNA. *Kpn*I and *Sma*I sites were introduced into the 5′- and 3′-termini, respectively, of the amplified fragment, which then was subcloned into the *Kpn*I–*Sma*I site of PGVB2 (Nippon Gene, Tokyo, Japan); the resulting reporter construct was termed PGVArom.

To construct a reporter plasmid containing an RXRE and RAR response element, response elements were cloned into the *Sma*I site of pTAL-Luc (CLONTECH Laboratories, Inc., Palo Alto, CA); response elements with the *underlined* consensus hexanucleotide sequence were as follows: DR1 × 2 (5′-AGGTCA a AGGTCA a AGGTCA a AGGTCA-3′); DR2 × 2 (5′- aa AGGTCA aa AGGTCA ccatcccgggaaa AGGTCA aa AGGTCA cc-3′); DR5 × 2 (5′-aa AGGTCA ccgaa AGGTCA ccatcccgggaaa AGGTCA ccgaa AGGTCA cc-3′); the resulting reporter constructs were termed pTALDR1, pTALDR2, and pTALDR5, respectively. The LBDs of hRXRα (codons 201–693), hRXRβ (codons 275–534), and hRXRγ (codons 172–455) were amplified by RT-PCR using mRNA from human liver and kidney and subcloned into pGEX-4T (Amersham Biosciences, Piscataway, NJ). These constructs were used for generation of glutathione *S*-transferase (GST)-hRXR fusion proteins. For chimeric receptor assay, the LBD of hRXRα was fused to the C-terminal end of GAL4-DNA binding domain (amino acids 1–147) in the pBK-CMV expression vector (Stratagene, La Jolla, CA) to yield pBK-CMV-GAL4-hRXRα. All sequences synthesized by PCR were confirmed by DNA sequencing. The plasmid p4×UAS-tk-luc, a LUC reporter construct containing four copies of the GAL4 binding site [upstream activating sequence (UAS) of GAL1] followed by a thymidine kinase promoter, was a kind gift from Dr. Y. Kamei (National Institute of Health and Nutrition, Japan).

Transient Transfection Assay

Transfection was performed with Lipofectamine regent (Invitrogen) in accordance with the manufacturer's instructions. JEG-3 cells (3×10^4 cells) were seeded in 24-well plates 24 h before transfection with the optimal dose of each DNA construct. At 18 h after transfection, various compounds were added to the transfected cells, which were then cultured in regular culture medium supplemented with 1% charcoal-stripped FCS instead of 10% normal FCS. The cells were harvested 30 h later, and extracts were prepared and assayed for LUC activity by using the dual-LUC reporter assay system (Promega Corp., Madison, WI) in accordance with the manufacturer's instructions. To normalize LUC activity for transfection and harvesting efficiency, the *Renilla* LUC control reporter construct pRL-TK (Promega) was cotransfected as an internal standard in all reporter experiments. The results are expressed as the average relative LUC activity of at least quadruplicate samples.

Ligand Binding Assay

The GST-RXR fusions were expressed in *Escherichia coli* DH5α cells and purified according to the manufacturer's (Amersham Biosciences) instructions. The purified proteins (30 μg/ml) were incubated with increasing concentrations of either [^{3}H]9cRA (1.63 tBq/mmol, Amersham Biosciences) or [^{14}C]TPTOH (2.04 gBq/mmol, Amersham Biosciences) with or without a 100-fold molar excess of each unlabeled compound. After incubation at 4 C for 1 h, specific binding was

determined by hydroxyapatite binding assay as described elsewhere (68). Binding in the presence of a 100-fold molar excess of unlabeled ligand was defined as nonspecific binding; specific binding was defined as total binding minus nonspecific binding. Similarly, tin compounds were used to compete for [^{3}H]9cRA and [^{14}C]TPTOH in this assay to determine the binding preferences of RXRs.

Statistics

Data were analyzed by the two-tailed unpaired Student's *t* test by using SPSS software (SPSS, Inc., Chicago, IL). Control and treatment group data were always obtained from equal numbers of replicate experiments. Values with $P < 0.05$ were considered statistically significant.

Acknowledgments

We thank Dr. Y. Kamei (National Institute of Health and Nutrition, Tokyo, Japan) for providing the plasmid p4xUAS-tk-luc and Teikoku Hormone Manufacturing (Tokyo, Japan) for the standardized hCG for ELISA.

Received October 7, 2004. Accepted June 1, 2005.

Address all correspondence and requests for reprints to: Dr. Tsuyoshi Nakanishi, Department of Toxicology, Graduate School of Pharmaceutical Sciences, Osaka University, 1–6, Yamadaoka Suita, Osaka 565-0871, Japan. E-mail: nakanishi@phs.osaka-u.ac.jp.

This work was supported in part by grants from a Grant in Aid for Scientific Research (nos. 13470499 and 15201012) from the Ministry of Education, Science, Sports, and Culture of Japan; Industrial Technology Research Grant Program in 2001 from New Energy and Industrial Technology Development Organization of Japan; Health and Labor Sciences Research Grants (Research on Advanced Medical Technology) from the Ministry of Health, Labor and Welfare of Japan; and The Long-Range Research Initiative, Japan.

REFERENCES

1. Chambon P 1996 A decade of molecular biology of retinoic acid receptors. FASEB J 10:940–954
2. Aranda A, Pascual A 2001 Nuclear hormone receptors and gene expression. Physiol Rev 81:1269–1304
3. Giguere V 1994 Retinoic acid receptors and cellular retinoid binding proteins: complex interplay in retinoid signaling. Endocr Rev 15:61–79
4. Sapin V, Ward SJ, Bronner S, Chambon P, Dolle P 1997 Differential expression of transcripts encoding retinoid binding proteins and retinoic acid receptors during placentation of the mouse. Dev Dyn 208: 199–210
5. Sapin V, Dolle P, Hindelang C, Kastner P, Chambon P 1997 Defects of the chorioallantoic placenta in mouse RXRα null fetuses. Dev Biol 191:29–41
6. Wendling O, Chambon P, Mark M 1999 Retinoid X receptors are essential for early mouse development and placentogenesis. Proc Natl Acad Sci USA 96: 547–551
7. Mascrez B, Mark M, Krezel W, Dupe V, LeMeur M, Ghyselinck NB, Chambon P 2001 Differential contributions of AF-1 and AF-2 activities to the developmental functions of RXRα. Development 128:2049–2062
8. Noback CR, Takahashi YI 1978 Micromorphology of the placenta of rats reared on marginal vitamin-A-deficient diet. Acta Anat (Basel) 102:195–202
9. Guibourdenche J, Alsat E, Soncin F, Rochette-Egly C, Evain-Brion D 1998 Retinoid receptors expression in human term placenta: involvement of RXRα in retinoid induced-hCG secretion. J Clin Endocrinol Metab 83: 1384–1387
10. Guibourdenche J, Roulier S, Rochette-Egly C, Evain-Brion D 1998 High retinoid X receptor expression in JEG-3 choriocarcinoma cells: involvement in cell function modulation by retinoids. J Cell Physiol 176: 595–601
11. Roulier S, Rochette-Egly C, Rebut-Bonneton C, Porquet D, Evain-Brion D 1994 Nuclear retinoic acid receptor characterization in cultured human trophoblast cells: effect of retinoic acid on epidermal growth factor receptor expression. Mol Cell Endocrinol 105:165–173
12. Matsuo H, Strauss III JF 1994 Peroxisome proliferators and retinoids affect JEG-3 choriocarcinoma cell function. Endocrinology 135:1135–1145
13. Sun T, Zhao Y, Mangelsdorf DJ, Simpson ER 1998 Characterization of a region upstream of exon I. 1 of the human CYP19 (aromatase) gene that mediates regulation by retinoids in human choriocarcinoma cells. Endocrinology 139:1684–1691
14. Tarrade A, Schoonjans K, Guibourdenche J, Bidart JM, Vidaud M, Auwerx J, Rochette-Egly C, Evain-Brion D 2001 PPARγ/RXRα heterodimers are involved in human CGβ synthesis and human trophoblast differentiation. Endocrinology 142:4504–4514
15. Zhu SJ, Li Y, Li H, Wang YL, Xiao ZJ, Vihko P, Piao YS 2002 Retinoic acids promote the action of aromatase and 17β-hydroxysteroid dehydrogenase type 1 on the biosynthesis of 17β-estradiol in placental cells. J Endocrinol 172:31–43
16. Simpson ER, Mahendroo MS, Means GD, Kilgore MW, Hinshelwood MM, Graham-Lorence S, Amarneh B, Ito Y, Fisher CR, Michael MD, Mendelson CR, Bulun SE 1994 Aromatase cytochrome P450, the enzyme responsible for estrogen biosynthesis. Endocr Rev 15: 342–355
17. Albrecht ED, Pepe GJ 1990 Placental steroid hormone biosynthesis in primate pregnancy. Endocr Rev 11: 124–150
18. Shozu M, Akasofu K, Harada T, Kubota Y 1991 A new cause of female pseudohermaphroditism: placental aromatase deficiency. J Clin Endocrinol Metab 72: 560–566
19. Yoshimi T, Strott CA, Marshall JR, Lipsett MB 1969 Corpus luteum function in early pregnancy. J Clin Endocrinol Metab 29:225–230
20. Huhtaniemi IT, Korenbrot CC, Jaffe RB 1977 hCG binding and stimulation of testosterone biosynthesis in the human fetal testis. J Clin Endocrinol Metab 44: 963–967
21. Boyer IJ 1989 Toxicity of dibutyltin, tributyltin and other organotin compounds to humans and to experimental animals. Toxicology 55:253–298
22. Fent K 1996 Ecotoxicology of organotin compounds. Crit Rev Toxicol 26:1–117
23. Horiguchi T, Shiraishi H, Shimizu M, Morita M 1997 Effects of triphenyltin chloride and five other organotin compounds on the development of imposex in the rock shell, *Thais clavigera.* Environ Pollut 95:85–91
24. Matthiessen P, Gibbs PE 1998 Critical appraisal of the evidence for tributyltin-mediated endocrine disruption in mollusks. Environ Toxicol Chem 17:37–43
25. Kannan K, Tanabe S, Iwata H, Tatsukawa R 1995 Butyltins in muscle and liver of fish collected from certain Asian and Oceanian countries. Environ Pollut 90:279–290
26. Kannan K, Tanabe S, Tatsukawa R 1995 Occurrence of butyltin residues in certain foodstuffs. Bull Environ Contam Toxicol 55:510–516

27. Nakanishi T, Kohroki J, Suzuki S, Ishizaki J, Hiromori Y, Takasuga S, Itoh N, Watanabe Y, Utoguchi N, Tanaka K 2002 Trialkyltin compounds enhance human CG secretion and aromatase activity in human placental choriocarcinoma cells. J Clin Endocrinol Metab 87:2830–2837
28. Chen CW, Hurd C, Vorojeikina DP, Arnold SF, Notides AC 1997 Transcriptional activation of the human estrogen receptor by DDT isomers and metabolites in yeast and MCF-7 cells. Biochem Pharmacol 53: 1161–1172
29. Korach KS, Sarver P, Chae K, McLachlan JA, McKinney JD 1988 Estrogen receptor-binding activity of polychlorinated hydroxybiphenyls: conformationally restricted structural probes. Mol Pharmacol 33: 120–126
30. Krishnan AV, Stathis P, Permuth SF, Tokes L, Feldman D 1993 Bisphenol-A: an estrogenic substance is released from polycarbonate flasks during autoclaving. Endocrinology 132:2279–2286
31. Kuiper GG, Lemmen JG, Carlsson B, Corton JC, Safe SH, van der Saag PT, van der Burg B, Gustafsson JA 1998 Interaction of estrogenic chemicals and phytoestrogens with estrogen receptor β. Endocrinology 139:4252–4263
32. Moore M, Mustain M, Daniel K, Chen I, Safe S, Zacharewski T, Gillesby B, Joyeux A, Balaguer P 1997 Antiestrogenic activity of hydroxylated polychlorinated biphenyl congeners identified in human serum. Toxicol Appl Pharmacol 142:160–168
33. Routledge EJ, Sumpter JP 1997 Structural features of alkylphenolic chemicals associated with estrogenic activity. J Biol Chem 272:3280–3288
34. White R, Jobling S, Hoare SA, Sumpter JP, Parker MG 1994 Environmentally persistent alkylphenolic compounds are estrogenic. Endocrinology 135:175–182
35. Kliewer SA, Umesono K, Noonan DJ, Heyman RA, Evans RM 1992 Convergence of 9-cis retinoic acid and peroxisome proliferator signalling pathways through heterodimer formation of their receptors. Nature 358: 771–774
36. Issemann I, Prince RA, Tugwood JD, Green S 1993 The peroxisome proliferator-activated receptor:retinoid X receptor heterodimer is activated by fatty acids and fibrate hypolipidaemic drugs. J Mol Endocrinol 11:37–47
37. Bardot O, Aldridge TC, Latruffe N, Green S 1993 PPAR-RXR heterodimer activates a peroxisome proliferator response element upstream of the bifunctional enzyme gene. Biochem Biophys Res Commun 192: 37–45
38. Westin S, Kurokawa R, Nolte RT, Wisely GB, McInerney EM, Rose DW, Milburn MV, Rosenfeld MG, Glass CK 1998 Interactions controlling the assembly of nuclear-receptor heterodimers and co-activators. Nature 395:199–202
39. Schulman IG, Shao G, Heyman RA 1998 Transactivation by retinoid X receptor-peroxisome proliferator-activated receptor γ (PPAR γ) heterodimers: intermolecular synergy requires only the PPAR γ hormone-dependent activation function. Mol Cell Biol 18:3483–3494
40. Laffitte BA, Kast HR, Nguyen CM, Zavacki AM, Moore DD, Edwards PA 2000 Identification of the DNA binding specificity and potential target genes for the farnesoid X-activated receptor. J Biol Chem 275: 10638–10647
41. Germain P, Iyer J, Zechel C, Gronemeyer H 2002 Co-regulator recruitment and the mechanism of retinoic acid receptor synergy. Nature 415:187–192
42. Allenby G, Bocquel MT, Saunders M, Kazmer S, Speck J, Rosenberger M, Lovey A, Kastner P, Grippo JF, Chambon P, Levin AA 1993 Retinoic acid receptors and retinoid X receptors: interactions with endogenous retinoic acids. Proc Natl Acad Sci USA 90:30–34
43. Sebastian S, Bulun SE 2001 A highly complex organization of the regulatory region of the human CYP19 (aromatase) gene revealed by the Human Genome Project. J Clin Endocrinol Metab 86:4600–4602
44. Bulun SE, Sebastian S, Takayama K, Suzuki T, Sasano H, Shozu M 2003 The human CYP19 (aromatase P450) gene: update on physiologic roles and genomic organization of promoters. J Steroid Biochem Mol Biol 86:219–224
45. Jameson JL, Hollenberg AN 1993 Regulation of chorionic gonadotropin gene expression. Endocr Rev 14: 203–221
46. Jameson JL, Lindell CM, Habener JF 1987 Gonadotropin and thyrotropin α- and β-subunit gene expression in normal and neoplastic tissues characterized using specific messenger ribonucleic acid hybridization probes. J Clin Endocrinol Metab 64:319–327
47. Saitoh M, Yanase T, Morinaga H, Tanabe M, Mu YM, Nishi Y, Nomura M, Okabe T, Goto K, Takayanagi R, Nawata H 2001 Tributyltin or triphenyltin inhibits aromatase activity in the human granulosa-like tumor cell line KGN. Biochem Biophys Res Commun 289: 198–204
48. Mu YM, Yanase T, Nishi Y, Takayanagi R, Goto K, Nawata H 2001 Combined treatment with specific ligands for PPARγ:RXR nuclear receptor system markedly inhibits the expression of cytochrome P450arom in human granulosa cancer cells. Mol Cell Endocrinol 181:239–248
49. Mu YM, Yanase T, Nishi Y, Waseda N, Oda T, Tanaka A, Takayanagi R, Nawata H 2000 Insulin sensitizer, troglitazone, directly inhibits aromatase activity in human ovarian granulosa cells. Biochem Biophys Res Commun 271:710–713
50. Thompson PD, Jurutka PW, Haussler CA, Whitfield GK, Haussler MR 1998 Heterodimeric DNA binding by the vitamin D receptor and retinoid X receptors is enhanced by 1,25-dihydroxyvitamin D3 and inhibited by 9-cis-retinoic acid. Evidence for allosteric receptor interactions. J Biol Chem 273:8483–8491
51. Forman BM, Umesono K, Chen J, Evans RM 1995 Unique response pathways are established by allosteric interactions among nuclear hormone receptors. Cell 81:541–550
52. Castillo AI, Sanchez-Martinez R, Moreno JL, Martinez-Iglesias OA, Palacios D, Aranda A 2004 A permissive retinoid X receptor/thyroid hormone receptor heterodimer allows stimulation of prolactin gene transcription by thyroid hormone and 9-cis-retinoic acid. Mol Cell Biol 24:502–513
53. Lala DS, Mukherjee R, Schulman IG, Koch SS, Dardashti LJ, Nadzan AM, Croston GE, Evans RM, Heyman RA, 1996 Activation of specific RXR heterodimers by an antagonist of RXR homodimers. Nature 383: 450–453
54. Kimmel EC, Fish RH, Casida JE 1976 Bioorganotin chemistry. Metabolism of organotin compounds in microsomal monooxygenase systems and in mammals. J Agric Food Chem 25:1–9
55. Ohhira S, Matsui H 2003 Metabolism of a tetraphenyltin compound in rats after a single oral dose. J Appl Toxicol 23:31–35
56. Ohhira S, Watanabe M, Matsui H 2003 Metabolism of tributyltin and triphenyltin by rat, hamster and human hepatic microsomes. Arch Toxicol 77:138–144
57. Unsworth B, Hennen S, Krishnakumaran A, Ting P, Hoffman N 1974 Teratogenic evaluation of terpenoid derivatives. Life Sci 15:1649–1655

58. de Urquiza AM, Liu S, Sjoberg M, Zetterstrom RH, Griffiths W, Sjovall J, Perlmann T 2000 Docosahexaenoic acid, a ligand for the retinoid X receptor in mouse brain. Science 290:2140–2144
59. Goldstein JT, Dobrzyn A, Clagett-Dame M, Pike JW, DeLuca HF 2003 Isolation and characterization of unsaturated fatty acids as natural ligands for the retinoid-X receptor. Arch Biochem Biophys 420:185–193
60. Harmon MA, Boehm MF, Heyman RA, Mangelsdorf DJ 1995 Activation of mammalian retinoid X receptors by the insect growth regulator methoprene. Proc Natl Acad Sci USA 92:6157–6160
61. Kitareewan S, Burka LT, Tomer KB, Parker CE, Deterding LJ, Stevens RD, Forman BM, Mais DE, Heyman RA, McMorris T, Weinberger C 1996 Phytol metabolites are circulating dietary factors that activate the nuclear receptor RXR. Mol Biol Cell 7:1153–1166
62. Lemotte PK, Keidel S, Apfel CM 1996 Phytanic acid is a retinoid X receptor ligand. Eur J Biochem 236: 328–333
63. Kagechika H 2002 Novel synthetic retinoids and separation of the pleiotropic retinoidal activities. Curr Med Chem 9:591–608
64. Egea PF, Mitschler A, Moras D 2002 Molecular recognition of agonist ligands by RXRs. Mol Endocrinol 16: 987–997
65. Benya TJ 1997 Bis(tributyltin) oxide toxicology. Drug Metab Rev 29:1189–1284
66. Watanabe H, Adachi R, Hirayama A, Kasahara T, Suzuki K 2003 Triphenyltin enhances the neutrophilic differentiation of promyelocytic HL-60 cells. Biochem Biophys Res Commun 306:26–31
67. Yamabe Y, Hoshino A, Imura N, Suzuki T, Himeno S 2000 Enhancement of androgen-dependent transcription and cell proliferation by tributyltin and triphenyltin in human prostate cancer cells. Toxicol Appl Pharmacol 169:177–184
68. Clagett-Dame M, Repa JJ 1997 Generating and characterizing retinoid receptors from *Escherichia coli* and insect cell expression systems. Methods Enzymol 282:13–24

Molecular Endocrinology **is published monthly by The Endocrine Society (http://www.endo-society.org), the foremost professional society serving the endocrine community.**

SETAC PRESS

Environmental Toxicology and Chemistry, Vol. 24, No. 8, pp. 1896–1901, 2005

Printed in the USA
0730-7268/05 $12.00 + .00

BIODEGRADATION OF BISPHENOL A AND DISAPPEARANCE OF ITS ESTROGENIC ACTIVITY BY THE GREEN ALGA *CHLORELLA FUSCA* VAR. *VACUOLATA*

TAKASHI HIROOKA,† HIROYASU NAGASE,*† KOTARO UCHIDA,† YUJI HIROSHIGE,† YOSHIE EHARA,† JUN-ICHI NISHIKAWA,‡ TSUTOMU NISHIHARA,‡ KAZUHISA MIYAMOTO,† and ZAZUMASA HIRATA,†
†Laboratory of Environmental Biotechnology, Graduate School of Pharmaceutical Sciences, Osaka University, 1-6 Yamadaoka, Suita, Osaka 565-0871, Japan
‡Laboratory of Environmental Biochemistry, Graduate School of Pharmaceutical Sciences, Osaka University, 1-6 Yamadaoka, Suita, Osaka 565-0871, Japan

(*Received* 20 *May* 2004; *Accepted* 2 *February* 2005)

Abstract—Bisphenol A (BPA) is known as an endocrine disruptor and often is found in landfill leachates. Removal of BPA by green alga, *Chlorella fusca*, was characterized, because we previously found that various phenols were well removed by this strain, including BPA. *Chlorella fusca* was able to remove almost all BPA in the concentration range from 10 to 80 μM for 168 h under continuous illumination at 18 W/m². At the low light intensity of 2 W/m², 82% of 40 μM BPA was removed, and only 27% was removed in the dark. Moreover, *C. fusca* could remove 90% of 40 μM BPA under the 8:16-h light:dark condition, which was almost as high as that under the continuous-light condition. The amount of BPA contained in the cells was less than the amount of BPA removed from the medium. Monohydroxybisphenol A was detected as an intermediate of BPA degradation. Moreover, estrogenic activity that originated from BPA in the culture medium also completely disappeared. Based on these results, BPA was finally degraded to compounds having nonestrogenic activity. Therefore, *C. fusca* can be considered a useful organism to remove BPA from landfill leachates.

Keywords—Bisphenol A *Chlorella fusca* Estrogenic activity Landfill leachate Monohydroxybisphenol A

INTRODUCTION

Microalgae frequently have been used in processes for removing pollutants, such as nitrogen and phosphorus, from wastewaters [1]. Biosorption of heavy metals and biodegradation of hazardous organic compounds by microalgae also have been reported [2,3]. In a previous study, we found that the green alga, *Chlorella fusca* var. *vacuolata* IAM C-28, which was obtained from the Institute of Applied Microbiology Culture Collection (Tokyo, Japan), could remove various kinds of phenols, such as chlorophenols, nitrophenols, and bisphenol A (BPA; 2,2-bis(4-hydroxyphenyl)propane), from medium [4].

Recently, BPA has often been detected in aquatic and soil environments [5,6]. Bisphenol A has an acute toxicity to aquatic organisms. It was reported that a median lethal concentration for fish is 3 to 15 mg/L and that a median effective concentration for green algae is 1 to 3 mg/L [6]. Because BPA also has endocrine-disrupting activity, it is hazardous to animals even at low concentrations [7,8]. Bisphenol A is widely used as a material to produce polycarbonate, epoxy resins, flame retardants, and other products. These plastics are finally disposed of into landfills, and BPA often is detected in landfill leachates at higher concentrations than those in environmental water [9,10]. Therefore, leachates are thought to be significant sources of BPA in aquatic environments. In Japan, landfill sites are categorized into three types depending on waste contents. Waste plastics, rubber, glasses, ceramics, nontoxic metals, and construction scrap materials are disposed of into landfill sites for stable industrial wastes. Industrial wastes containing toxic substances at high level are disposed of into strictly controlled landfills for industrial wastes. The other industrial and domestic wastes are disposed of into leachate-controlled landfills equipped with a leachate-treatment system. Urase et al. [11] and Yamada et al. [12] reported that more than 90% of the BPA contained in leachates from controlled-type landfill sites was removed by treatment processes consisting of activated sludge method, coagulation, sedimentation, sand filtration, and activated carbon adsorption. However, BPA also is detected in leachate from landfill sites for stable industrial wastes, which are not equipped with a leachate-treatment system [11,12]. Because the cost of the usual leachate-treatment system is high, a low-cost treatment system is required to remove BPA in leachates from open-landfill sites.

The present report focuses on the utilization of microalgae for removing BPA from landfill leachates. We evaluated the ability of *C. fusca* to remove BPA in batch experiments under light, dark, and light-dark cycle conditions. We also investigated the degradation of BPA by the cells, and then we identified an intermediate of BPA degradation. The disappearance of estrogenic activity originated from BPA in the culture medium also was analyzed by the yeast two-hybrid assay [13].

MATERIALS AND METHODS

Microorganism and culture condition

Chlorella fusca was precultivated in a modified Bristol medium at 27.5°C under continuous illumination with white fluorescent light at an intensity of 18 W/m² and aerated with air containing 1% CO_2. After 7 d, cells were harvested and inoculated into a 100-ml glass test tube as described previously [4]. Algal cells were cultivated under the same conditions as used for precultivation with 40 μM BPA as basal condition for BPA removal. To evaluate the ability of *C. fusca* for BPA

* To whom correspondence may be addressed (nagase@phs.osaka-u.ac.jp).

removal, the BPA concentration was varied from 10 to 160 μM. To examine the effect of illuminating conditions on BPA removal, the light intensity was changed from 0 to 36 W/m² at the surface of the glass test tube, and the effect of a light-dark cycle (8:16-h light:dark photoperiod; light intensity, 18 W/m²) also was investigated. The concentration of BPA and the cell density were measured every 24 h after addition of BPA. All the batch experiments were undertaken in triplicate.

Analytical methods

The cell growth was evaluated by the optical density at 680 nm and measured by a spectrophotometer (U-2000; Hitachi, Tokyo, Japan). The concentration of BPA was measured using a high-performance liquid chromatography (HPLC) system (D-7000 series; Hitachi) with a diode-array detector (L-4500; Hitachi) at 280 nm. The pretreatment method for the HPLC sample was as follows: The culture (2 ml) was centrifuged (11,000 *g*, 4°C, 5 min), 200 μl of the supernatant were mixed with 20 μl of 6 N HCl to remove proteins, and a second centrifugation was performed (17,360 *g*, 4°C, 11 min). The supernatant (40 μl) was then injected into the HPLC system, which was equipped with a reversed-phase column (250 × 4.6 mm I. D., 5 mm; Mightysil RP-18; Kanto Chemical, Tokyo, Japan). Acetonitrile/50 mM potassium dihydrogenphosphate buffer (pH 2.5; 50/50 [v/v]) was used as the mobile phase at a flow rate of 0.7 ml/min. Degradation intermediates of BPA were identified using the HPLC–mass spectrometry (LC-MS) system (LCQ Advantage; Thermo Finnigan, San Jose, CA, USA) with an electrospray ionization interface. The HPLC sample (50 μl) was injected into the LC-MS system equipped with a reversed-phase column (250 × 4.6 mm I. D., 5 mm; L-column; Chemical Evaluation and Research Institute, Tokyo, Japan). Water/acetonitrile (60/40 [v/v]) was used as the mobile phase at a flow rate of 1.0 ml/min. The electrospray ionization interface was operated in a negative-ion mode.

Extraction of BPA from algal cells

Chlorella fusca was cultivated in the presence of 40 μM BPA in the light at 18 W/m². Algal cells were harvested from 5 ml of culture by centrifugation (845 *g*, 5°C, 5 min) and washed three times with distilled water. Cell pellets were resuspended in 5 ml of distilled water. After ultrasonic disruption (Sonifier 450; Branson, Danbury, CT, USA) of the cells, 12.5 ml of methanol and 6.25 ml of chloroform were added. This solution was shaken for 1 h. Next, 6.25 ml of distilled water and 6.25 ml of chloroform were added to the solution, and the organic phase was collected by centrifugation (845 *g*, 5°C, 5 min). This treatment was repeated four times. Chloroform was evaporated completely from the organic phase by a rotary evaporator. The residual matter was dissolved in 10 ml of methanol and then analyzed by HPLC.

Chemical oxidation of BPA by Fremy's salt

Bisphenol A was oxidized by potassium nitrosodisulfonate (Fremy's salt; Sigma-Aldrich, St. Louis, MO, USA) to prepare monohydroxybisphenol A according to a previously reported method [14]. Fremy's salt (0.1 g) was added to 66 ml of 25 mM sodium dihydrogenphosphate buffer solution containing 13 mM BPA in a 200-ml Erlenmeyer flask. The mixture was shaken for 20 min at 25°C and then extracted with chloroform. After the organic phase was collected and chloroform evaporated, the residual matter containing red crystals was dissolved in 10 ml of ethanol. The solution was analyzed by LC-MS.

Estrogenic activity of the culture supernatant

The estrogenic activity of the culture supernatant was estimated by a two-hybrid yeast assay using the recombinant yeast *Saccharomyces cerevisiae* Y190 with pGBT9-ER LBD and pGAD424-TIF2 as described by Nishikawa et al. [13] with some modifications. Then, 250 μl of the supernatant of the *C. fusca* culture containing BPA or of that containing ethanol as a negative control were mixed with 200 μl of synthetic dextrose medium. The yeast, which had been precultured for 48 h, was added to the mixture at a volume of 50 μl and then cultivated for 4 h at 30°C in a culture-tube rotator (LD-76; Labinco B.V., Breda, The Netherlands) at 30 rpm. After the optical density at 595 nm (OD_{595}) of the culture was measured, the yeast cells were collected by centrifugation (1,100 *g*, 4°C, 5 min) from 350 μl of the culture and then resuspended in 200 μl of Z buffer (pH 7.0) containing 21.49 g of $Na_2HPO_4 \cdot 12H_2O$, 6.22 g of $NaH_2PO_4 \cdot 2H_2O$, 0.75 g of KCl, 0.246 g of $MgSO_4 \cdot 7H_2O$, 0.27 ml of β-mercaptoethanol, and 1 g of Zymolyase 20T (Seikagaku, Tokyo, Japan) in 1 L. Samples were incubated for 15 min at 37°C, and then enzymatic reaction was started by adding 40 μl of 4 g/L *o*-nitrophenyl-β-D-galactopyranoside. The mixtures were incubated for 90 min at 30°C, and 100 μl of 1 M Na_2CO_3 were added to stop the reaction. After centrifugation (17,360 *g*, 4°C, 5 min), the absorbance of the supernatant at 415 and 550 nm (A_{415} and A_{550}, respectively) was measured. Estrogenic activity was indicated as β-galactosidase activity (U) calculated by the following equation:

$$U = (A_{415} - (1.75 \cdot A_{550})) \times 10^3/(t \cdot v \cdot OD_{595})$$

where t is the time of reaction (90 min) and v is the volume of mixture used in the assay (0.05 ml).

RESULTS

Effects of initial BPA concentration on its removal and algal growth

The effect of initial BPA concentration on its removal was investigated. The concentration of BPA in uninoculated media was found not to decrease (data not shown). *Chlorella fusca* was cultivated with BPA in the concentration range from 10 to 160 μM for 168 h under the continuous-light condition (18 W/m²). Figure 1 shows the BPA removal and cell growth. More than 95% of BPA was removed at the concentration between 10 and 80 μM, although only 70% of 160 μM BPA was removed. Therefore, it can be assumed that BPA was removed by the algal cells. This strain grew well in the BPA concentration range from 10 to 40 μM. Because the concentration of BPA in Japanese landfill leachates generally was lower than 40 μM [9–12], the initial BPA concentration was set at 40 μM for subsequent experiments.

Effects of light condition on BPA removal

To investigate the effects of light intensity on BPA removal, *C. fusca* was cultivated in the light-intensity range from 0 to 36 W/m² for 168 h (Fig. 2). The growth rates of this strain decreased with decreasing light intensity, and growth did not occur in the dark. The BPA removal was 98% at 36 W/m² and 82% at 2 W/m², although the removal decreased to 27% in the dark. Therefore, light illumination was an important parameter for achieving a high ability to remove BPA.

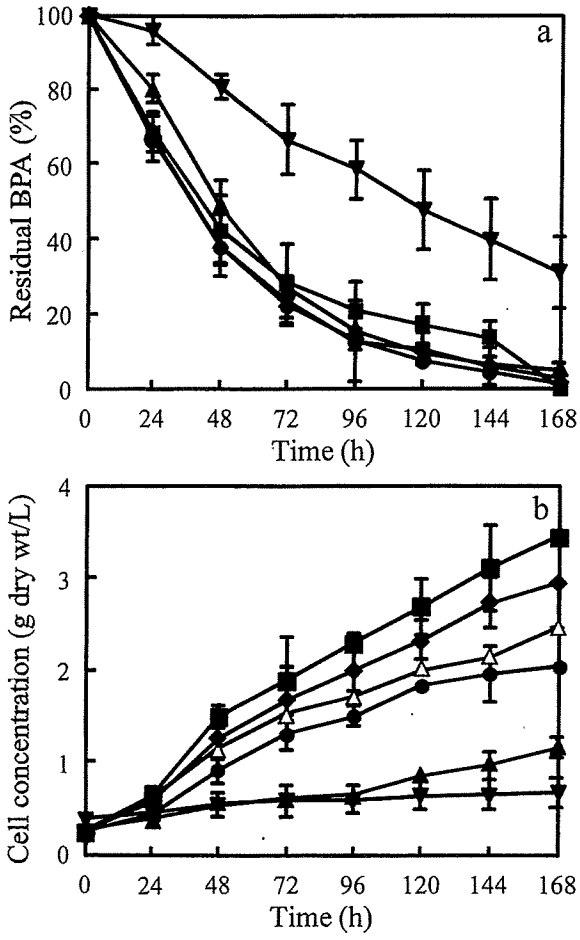

Fig. 1. Effect of initial bisphenol A (BPA) concentrations on its removal (**a**) and growth (**b**). The initial BPA concentrations were 0 μM (△), 10 μM (■), 20 μM (◆), 40 μM (●), 80 μM (▲), and 180 μM (▼). The light intensity was 18 W/m². Values were the averages of triplicate determinations. Error bars indicate standard deviations.

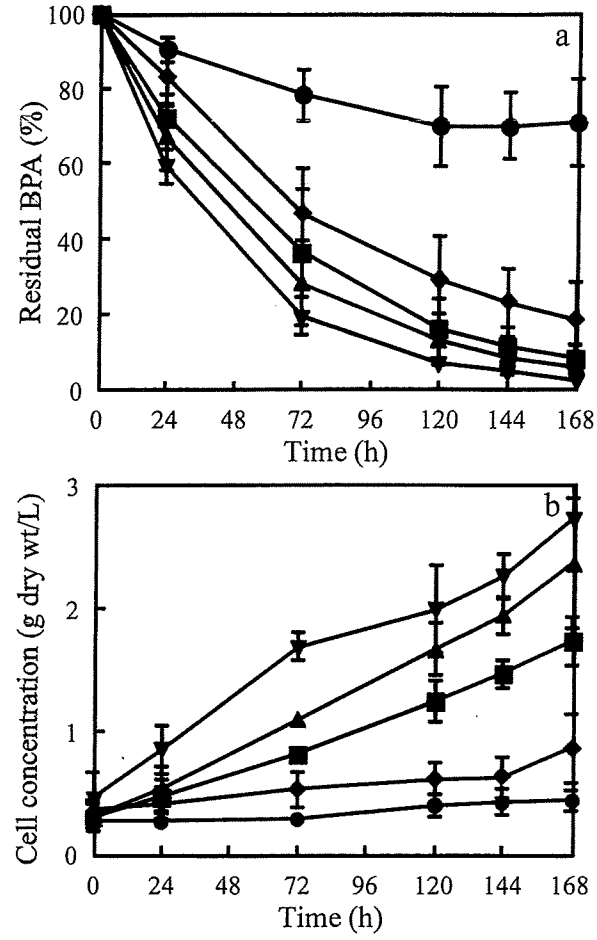

Fig. 2. Effect of light intensity on bisphenol A (BPA) removal (**a**) and growth (**b**). Light intensities tested were 0 W/m² (●), 2 W/m² (◆), 9 W/m² (■), 18 W/m² (▲), and 36 W/m² (▼). Values were the averages of triplicate determinations. Error bars indicate standard deviations.

Removal of BPA under the 8:16-h light:dark photoperiod (light intensity, 18 W/m²) also was investigated (Fig. 3). *Chlorella fusca* grew well and removed 90% of BPA, a result not very different from that obtained under continuous light (18 W/m²) for 168 h.

Biodegradation of BPA by C. fusca

To determine whether BPA was degraded by the cells or simply accumulated in the cells, the amount of BPA in the cells cultivated at 18 W/m² was analyzed (Fig. 4). The amount of BPA contained in the cells was significantly less than the amount of BPA removed from the medium. At the end of the cultivation time, BPA in the cells finally was decreased below the detection limit of HPLC analysis. This result indicates that BPA removal by *C. fusca* was caused by biodegradation by the cells rather than by simple accumulation in the cells.

On the HPLC chromatogram, an unknown peak at 8.2 min was observed in the culture medium in the light. A typical chromatogram is shown in Figure 5a. At 2 W/m², this peak area increased with decreasing BPA until 72 h and then decreased (data not shown). This peak was analyzed by LC-MS, and the mass spectrum of it revealed a parent-ion peak $[M-1]^-$ at *m/z* 243.11 (Fig. 6a). Because the molecular weight of BPA is 228.29, it was suggested that hydroxylation occurred in BPA. Based on these LC-MS results, this compound was thought to be monohydroxybisphenol A, an intermediate of BPA degradation by *C. fusca*. Atkinson and Roy [14] reported that monoquinone and monohydroxy derivatives of BPA were produced by BPA oxidation using Fremy's salt, strong oxidizing agent, and treatment with 1 N HCl. Therefore, monohydroxybisphenol A was produced according to their method and compared with the intermediate of BPA degraded by *C. fusca* using HPLC and LC-MS. The BPA degradation intermediate showed the same retention time (8.2 min) and mass spectrum as those of monohydroxybisphenol A (Figs. 5b and 6b).

Disappearance of estrogenic activity in the culture

To determine if estrogenic activity originated from BPA in the culture medium of *C. fusca* was decreased on BPA removal, the change of this activity was analyzed by yeast two-hybrid assay (Fig. 7). The activity decreased with decreasing BPA concentration and then completely disappeared.

DISCUSSION

In the present study, the green alga *C. fusca* well degraded BPA in the concentration range from 10 to 80 μM in the light (Fig. 1a). Yamamoto et al. [9] reported that the highest BPA concentration detected in landfill leachates was 75 μM, indicating that it is possible for *C. fusca* to remove BPA at this

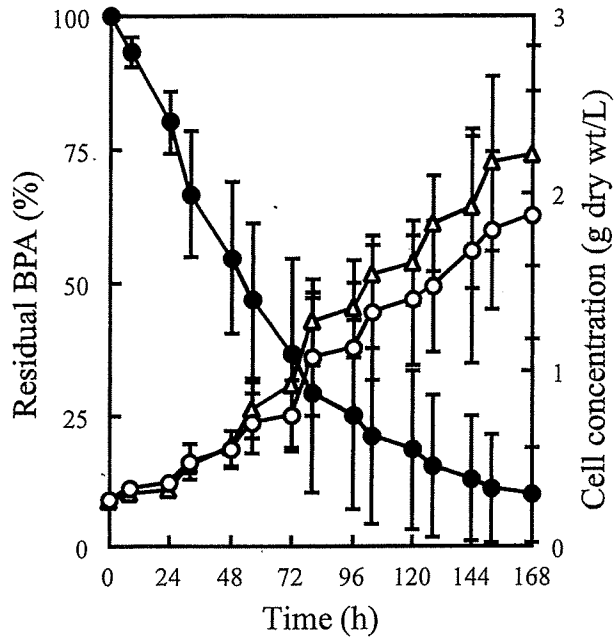

Fig. 3. Removal of bisphenol A (BPA) and growth under light-dark cycle condition. The BPA residual was shown (●). Algal cell concentration measured in media containing BPA (○) and not containing BPA (△), both incubated under 8:16-h light:dark photoperiod. Values were the averages of triplicate determinations. Error bars indicate standard deviations.

concentration. Several reports have appeared regarding the removal of BPA by bacteria. The gram-negative bacterium strain MV-1, isolated from the sludge of a wastewater treatment plant at a plastic manufacturing facility, was able to use BPA as a sole carbon and energy source. This bacterium removed 1.1 mM BPA completely from culture for 4 h [15]. Ronen and Abeliovich [16] reported that the gram-negative bacterium

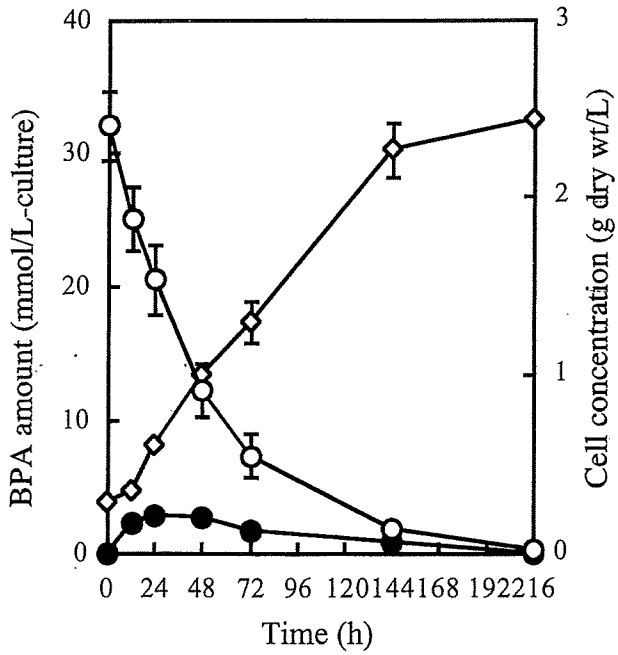

Fig. 4. Removal of bisphenol A (BPA) from the culture medium and change of its amount in the cells. Error bars indicate standard deviations. ○ = BPA amount in the culture medium; ● = BPA amount in cells; ◇ = cell amount.

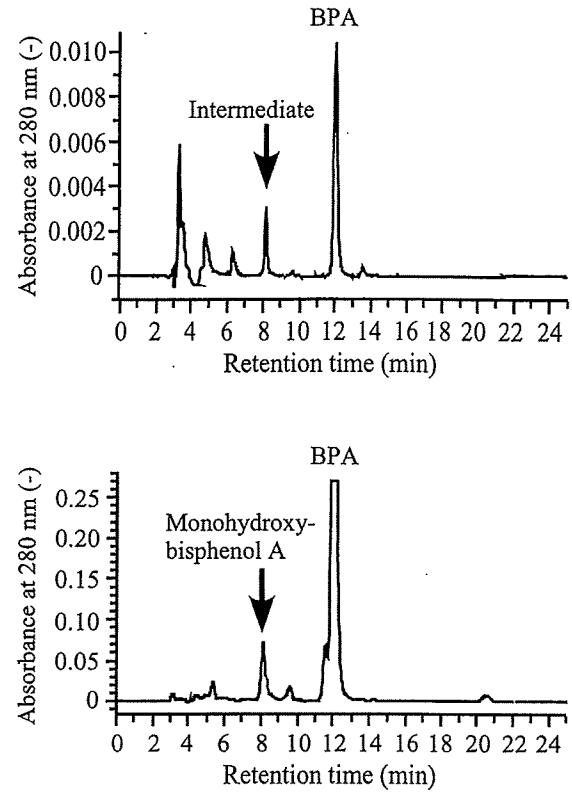

Fig. 5. High-performance liquid chromatograms of oxidized and degraded intermediate of bisphenol A (BPA) by *Chlorella fusca* (**top**) and Fremy's salt (**bottom**).

WH1, isolated from BPA-contaminated soil, removed 900 μM BPA completely from culture for 96 h. Kang and Kondo [17] reported that two *Pseudomonas* strains isolated from a river-water sample in Japan removed approximately 90% of 4 μM BPA for 240 h. However, these heterotrophic bacteria sometimes are difficult to use directly for treatment of BPA in landfill leachates, because the level of biologically available organic carbon sources usually is low. Therefore, it is necessary to add an external organic carbon source to maintain the biomass and the ability to remove BPA. On the other hand, microalgae can grow by using CO_2 as a carbon source. In this case, no need exists to supply any organic carbon sources. Therefore, *C. fusca* is thought to be useful to remove BPA contained in landfill leachates.

Chlorella fusca showed a high ability to remove BPA in the light-intensity range of 2 to 36 W/m^2, although this ability for removal decreased in the dark (Fig. 2). These results suggest that the light-illumination during cultivation is an important factor for the treatment of BPA by *C. fusca*. Bisphenol A also was removed in the light-dark cycle (Fig. 3), indicating that *C. fusca* would be a useful organism for BPA removal in the day-and-night cycle at most temperate or tropical outdoor sites.

As shown in Figure 4, the taken-up BPA was degraded in the cells. The degradation intermediate of BPA by *C. fusca* was identified as monohydroxybisphenol A, and this compound disappeared in the subsequent cultivation. Therefore, monohydroxybisphenol A would be a primary intermediate of BPA degradation in the light. In the case of bacteria, several intermediates of BPA degradation have been reported. The MV-1 strain has two pathways for BPA degradation [15,18]. The major pathway produces two primary intermediates, 4-

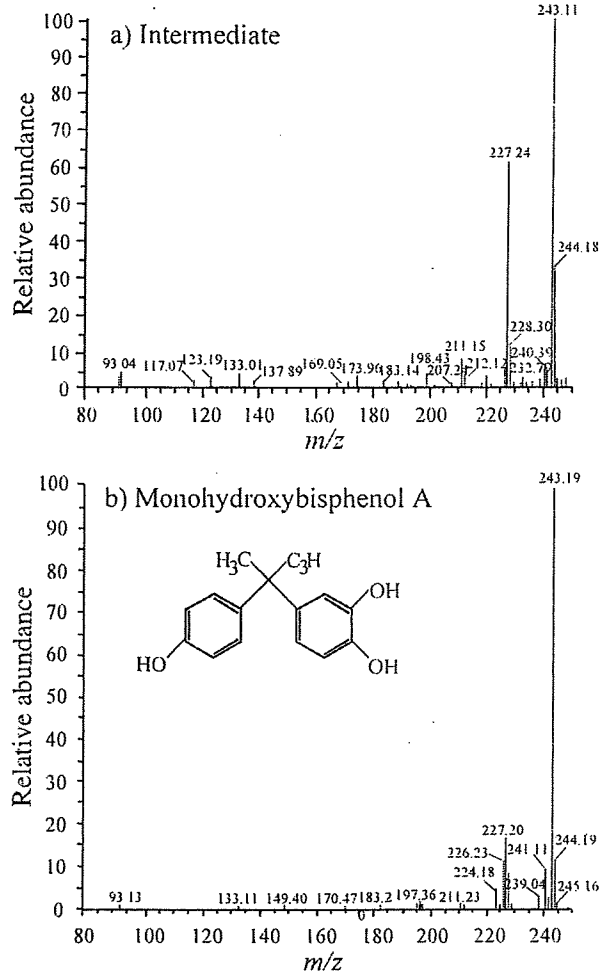

Fig. 6. Liquid chromatography–mass spectra of degraded intermediate of bisphenol A (BPA) by *Chlorella fusca* (**a**) and monohydroxybisphenol A (**b**).

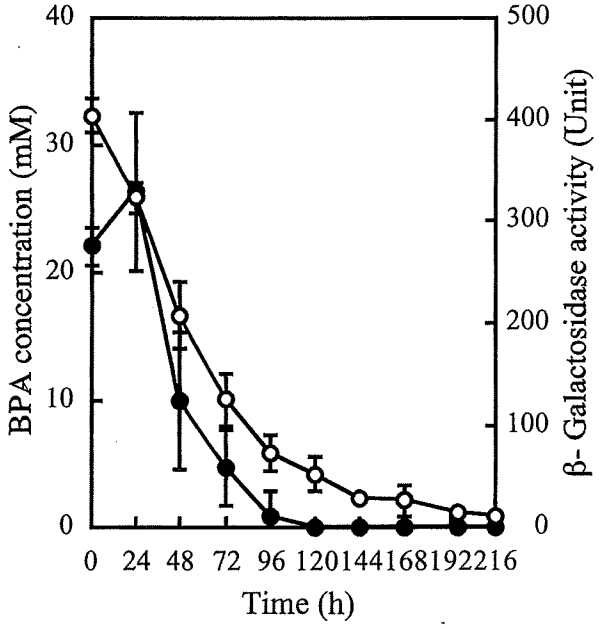

Fig. 7. Change of bisphenol A (BPA) concentration and estrogenic activity in the culture medium. Error bars indicate standard deviations. ○ = residual of BPA; ● = estrogenic activity in the culture medium.

hydroxybenzoic acid and 4-hydroxyacetophenone, and these intermediates were not detected in the case of *C. fusca*. On the other hand, monohydroxybisphenol A was reported as an intermediate of BPA degradation by potato (*Solanum tuberosum*) [19]. The BPA degradation pathway of *C. fusca* is similar to that in higher plants and not bacteria.

The reported degradation intermediates of BPA by heterotrophic bacteria have lower estrogenic activity compared with BPA [20]. The estrogenic activity also disappeared with the degradation of BPA by *C. fusca* (Fig. 7), indicating that *C. fusca* degrades BPA to intermediates with no estrogenic activity, including monohydroxybisphenol A. Therefore, it is possible to decrease the environmental effect of BPA using *C. fusca*.

The present study is, to our knowledge, the first to show that microalga *C. fusca* has the ability to degrade BPA. Microalgae have been employed to remove nitrogen and phosphorus in domestic wastewater by using a large-scale pond system. A similar system would be possible to remove BPA from landfill leachates, although further detailed studies will be required to achieve practical outdoor cultivation of *C. fusca* that maintain a high ability for BPA removal.

Acknowledgement—The present study was partly supported by a grant from the Heiwa Nakajima Foundation.

REFERENCES

1. Oswald WJ. 1988. Micro-algae and waste-water treatment. In Borowitzka MA, Borowitzka LJ, eds, *Micro-algal Biotechnology*. Cambridge University Press, New York, NY, USA, pp 305–328.
2. Nagase H, Inthorn D, Isaji Y, Oda A, Hirata K, Miyamoto K. 1997. Selective cadmium removal from hard water using NaOH-treated cells of the cyanobacterium *Tolypothrix tenuis*. *J Ferment Bioeng* 84:151–154.
3. Semple KT, Cain RB, Schmidt S. 1999. Biodegradation of aromatic compounds by microalgae. *FEMS Microbiol Lett* 170:291–300.
4. Hirooka T, Akiyama Y, Tsuji N, Nakamura T, Nagase H, Hirata K, Miyamoto K. 2003. Removal of hazardous phenols by microalgae under photoautotrophic conditions. *J Biosci Bioeng* 95: 200–203.
5. Lee HB, Peart TE. 2000. Determination of bisphenol A in sewage effluent and sludge by solid-phase and supercritical fluid extraction and gas chromatography/mass spectrometry. *J AOAC Int* 83: 290–297.
6. Staples CA, Dorn PB, Klecka GM, O'Block ST, Harris LR. 1998. A review of the environmental fate, effects, and exposures of bisphenol A. *Chemosphere* 36:2149–2173.
7. Dodds EC, Lawson W. 1936. Synthetic estrogenic agents without the phenanthrene nucleus. *Nature* 137:996.
8. Krishnan AV, Stathis P, Permuth SF, Tokes L, Feldman D. 1993. Bisphenol A: An estrogenic substance is released from polycarbonate flasks during autoclaving. *Endocrinology* 132:2279–2286.
9. Yamamoto T, Yasuhara A, Shiraishi H, Nakasugi O. 2001. Bisphenol A in hazardous waste landfill leachates. *Chemosphere* 42: 415–418.
10. Yasuhara A, Shiraishi H, Nishikawa M, Yamamoto T, Nakasugi O, Okumura T, Kenmotsu K, Fukui H, Nagase M, Kawagoshi Y. 1999. Organic components in leachates from hazardous waste disposal sites. *Waste Manag Res* 17:186–197.
11. Urase T, Miyashita K. 2003. Factors affecting the concentration of bisphenol A in leachates from solid waste disposal sites and its fate in treatment processes. *Journal of Material Cycles and Waste Management* 5:77–82.
12. Yamada K, Urase T, Matsuo T, Suzuki N. 1999. Constituents of organic pollutants in leachates from different types of landfill sites and their fate in the treatment processes. *Journal of Japan Society of Water Environment* 22:40–45.
13. Nishikawa J, Saito K, Goto J, Dakeyama F, Matsuo M, Nishihara T. 1999. New screening methods for chemicals with hormonal activities using interaction of nuclear hormone receptor with coactivator. *Toxicol Appl Pharmacol* 154:76–83.

14. Atkinson A, Roy D. 1995. In vitro conversion of environmental estrogenic chemical bisphenol A to DNA binding metabolite(s). *Biochem Biophys Res Commun* 210:424–433.
15. Lobos JH, Leib TK, Su T-M. 1992. Biodegradation of bisphenol A and other bisphenols by a gram-negative aerobic bacterium. *Appl Environ Microbiol* 58:1823–1831.
16. Ronen Z, Abeliovich A. 2000. Anaerobic-aerobic process for microbial degradation of tetrabromobisphenol A. *Appl Environ Microbiol* 66:2372–2377.
17. Kang J-H, Kondo F. 2002. Bisphenol A degradation by bacteria isolated from river water. *Arch Environ Contam Toxicol* 43:265–269.
18. Spivack J, Leib TK, Lobos JH. 1994. Novel pathway for bacterial metabolism of bisphenol A. *J Biol Chem* 269:7323–7329.
19. Xuan YJ, Endo Y, Fujimoto K. 2002. Oxidative degradation of bisphenol A by crude enzyme prepared from potato. *J Agric Food Chem* 50:6575–6578.
20. Ike M, Chen MY, Jin CS, Fujita M. 2002. Acute toxicity, mutagenicity, and estrogenicity of biodegradation products of bisphenol-A. *Environ Toxicol* 17:457–461.

2742–2750 Nucleic Acids Research, 2005, Vol. 33, No. 8
doi:10.1093/nar/gki560

Published online 12 May 2005

Chromatin assembly factor Asf1p-dependent occupancy of the SAS histone acetyltransferase complex at the silent mating-type locus *HMLα*

Shigehiro Osada*, Mitsumasa Kurita, Jun-ichi Nishikawa and Tsutomu Nishihara

Laboratory of Environmental Biochemistry, Graduate School of Pharmaceutical Sciences, Osaka University, 1-6 Yamada-Oka, Suita, Osaka 565-0871, Japan

Received January 28, 2005; Revised and Accepted April 20, 2005

ABSTRACT

Transcriptional repression of the silent mating-type loci *HMLα* and *HMR*a in *Saccharomyces cerevisiae* is regulated by chromatin structure. Sas2p is a catalytic subunit of the SAS histone acetyltransferase (HAT) complex. Although many HATs seem to relieve chromosomal repression to facilitate transcriptional activation, *sas* mutant phenotypes include loss of *SIR1*-dependent silencing of *HMLα*. To gain insight into the mechanism of the SAS complex mediated silencing at *HMLα*, we investigated the expression and chromatin structure of the α2 gene in the *HMLα* locus. We found that deletion of *SAS2* in combination with a null allele of *SIR1* changed the chromatin structure of the precisely positioned nucleosome, which includes the mRNA start site of the α2 gene and derepressed α2 transcription. The Sas2p HAT domain was required for this silencing. Furthermore, chromatin immunoprecipitation analysis revealed that the SAS complex was associated with the *HMLα* locus, and *ASF1* (which encodes chromatin assembly factor Asf1p), but not *SIR1* and *SIR2*, was necessary for this localization. These data suggest that the HAT activity and *ASF1*-dependent localization of the SAS complex are required for *SIR1*-dependent *HMLα* silencing.

INTRODUCTION

Silencing affects gene repression in a regional rather than promoter- or sequence-specific manner (1). The structure of the chromatin itself can affect gene expression, and changes in chromatin structure can result from the modification of histone tails as well as from the action of chromatin-remodeling complexes (2). A number of factors have been identified that contribute to transcriptional regulation by covalent modification of histones. In many cases, a relationship between histone acetylation and gene activation has been revealed by the identification of transcriptional co-activators, such as dedicated histone acetyltransferases (HATs) (3,4). Histone acetylation is reversed by histone deacetylases (HDACs), and many repression phenomena are regulated by HDACs (5). Moreover, HATs have been shown to contribute to repression and activation (4).

In *Saccharomyces cerevisiae*, silenced loci include the *HMLα* and *HMR*a mating-type loci, the telomere regions and the ribosomal DNA repeats (2). A variety of proteins, including the silent information regulator (Sir) proteins, are required to silence the mating information genes at silent loci (6). One of the Sir proteins, Sir2p, possesses HDAC activity important for silencing (7,8). Disruption of the *SIR2*, *SIR3* or *SIR4* gene results in loss of silencing at *HM* loci, and a *SIR1*-disrupted strain is composed of mixed populations of silenced and unsilenced cells (9).

Something About Silencing (*SAS*) *2* was identified as an enhancer of *sir1* epigenetic *HMLα* silencing defects (10). Sas2p is a member of the MYST (MOZ, Ybf2/Sas3, Sas2 and TIP60) family of HATs and forms a complex, termed the SAS complex, with Sas4p and Sas5p (11–14). The SAS complex mainly acetylates histone H4 at lysine 16 (12–16). The role of *SAS2* in silencing is different for each silenced locus. At *HMLα*, deletion of *SAS2* has very little effect on silencing. However, deletion of *SAS2* combined with deletion of *SIR1* causes a severe silencing defect (10,17). Normal *HMR*a silencing is unaffected by *SAS2* deletion, but *sas2* mutation suppresses the silencing defect caused by mutations in silencer elements of *HMR*a (10,17). To determine the role of *SAS2* in rDNA silencing, a strain in which the *URA3* gene is integrated at the rDNA locus was used. The *sas2* deletion strain showed more effective *URA3* repression, indicating that the deletion of *SAS2* increased rDNA repression (12). In the case of telomeres, loss of *SAS2* causes hypoacetylation in adjacent sub-telomeric regions, leading to the recruitment of

*To whom correspondence should be addressed. Tel: +81 6 6879 8242; Fax: +81 6 6879 8244; Email: osada@phs.osaka-u.ac.jp

Sir3p to these regions and inactivation of gene expression (15,16). Therefore, *sas2* mutations reduce silencing of *HMLα* (when combined with deletion of *SIR1*) but improve silencing at *HMR***a** when accompanied by a weakened silencer element, hypoacetylated sub-telomeric regions, or the rDNA locus. To understand the differing roles of Sas2p, it is important to investigate the biochemical mechanisms by which these factors regulate gene silencing in each silent locus.

We previously showed that the chromatin assembly factor Asf1p interacts with the SAS complex, and *ASF1* and *SAS2* genetically function in the same pathway to repress the *HMLα* locus (11). In the present study, we show that *SAS2* is essential for the organization of the chromatin structure at *HMLα* in a *sir1* mutant and that *ASF1* is required for the recruitment of the SAS complex to the *HMLα* locus.

MATERIALS AND METHODS

Yeast strains, plasmids and manipulations

The strains used in this study are listed in Table 1 and were either published previously or were created for this study by using standard yeast manipulations (18,19). Expression plasmids of wild-type and mutant alleles of *SAS2* and *ASF1* were described previously (11). Mating assays were performed as described previously (11,20).

Table 1. Yeast strains used in this study

Strain[a]	Genotype	Source
W303-1a	MATa *ade2-1 his3-11, 15 leu2-3, 112 trp1-1 ura3-1 can1-100*	J. Workman
W303-1b	MATα *ade2-1 his3-11, 15 leu2-3, 112 trp1-1 ura3-1 can1-100*	J. Workman
YJW228	a *SAS4-13Myc:kanMX6*	J. Workman
YJW229	a *SAS5-13Myc:kanMX6*	J. Workman
YJW252	a *sir1Δ::LEU2*	D. Rivier
YJW253	a *sas2Δ::TRP1*	D. Rivier
YJW257	a *sir4Δ::URA3 lys2Δ::hisG*	D. Rivier
YJW258	a *sas2Δ::TRP1 sir1Δ::LEU2*	D. Rivier
YJW265	a *SAS2-13Myc:HIS3MX6*	J. Workman
YJW269	a *SAS2-13Myc:HIS3MX6 sas4Δ::kan*	J. Workman
YJW270	a *SAS2-13Myc:kanMX6 sas5Δ::HIS3*	J. Workman
YJW271	a *SAS2-13Myc:TRP sas4Δ::kan sas5Δ::HIS3*	J. Workman
YJW433	a *asf1Δ::HIS3MX6*	J. Workman
YJW435	a *asf1Δ::HIS3 sir1Δ::LEU2*	J. Workman
YJW436	a *asf1Δ::HIS3 sas2Δ::TRP1*	J. Workman
YS480	a *sir3Δ::HIS3MX6*	
YSM64	a *sir2Δ::HIS3MX6*	
YSM85	a *SAS2-13Myc:kanMX6 sir1Δ::HIS3MX6*	
YSM87	a *SAS2-13Myc:kanMX6 asf1Δ::HIS3MX6*	
YSM90	a *SAS2-13Myc:kanMX6 sir2Δ::HIS3MX6*	
YSM104	a *SAS2-13Myc:kanMX6 asf1Δ::HIS3MX6 sir1Δ::TRP*	
YSM112	W303-1a [pRS416/CEN/URA3 (pS14)]	
YSM113	YJW265 [pRS416/CEN/URA3 (pS14)]	
YSM114	YSM87 [pRS416/CEN/URA 3(pS14)]	
YSM115	YSM87 [Ycp50/CEN/URA3/ASF1 (pLS27)]	
YSM116	YSM104 [pRS416/CEN/URA3 (pS14)]	
YSM117	YSM104 [Ycp50/CEN/URA3/ASF1 (pLS27)]	
YSM118	W303-1a [pRS416/CEN/URA3 (pS15)]	
YSM119	W303-1b [pRS416/CEN/URA3 (pS15)]	
YSM120	YJW252 [pRS416/CEN/URA3 (pS15)]	
YSM121	YJW258 [pRS416/CEN/URA3 (pS15)]	
YSM122	YJW258 [pRS416/CEN/URA3/ PSAS2-SAS2 (pS126)]	
YSM123	YJW258 [pRS416/CEN/URA3/ PSAS2-SAS2-M1 (pS136)]	
YJW251[b]	α *his4*	D. Rivier

[a]Strains, except YJW251, are isogenic with W303-1a or W303-1b.
[b]YJW251 is a lawn strain for mating assays.

RNA blots

A 40 μg aliquot of total RNA prepared from logarithmically growing cells was separated on 1.0% agarose–formaldehyde gels and transferred to Hybond-N+ membranes (Amersham Biosciences, Piscataway, NJ). Specific messages were detected using randomly labeled α2 and *SCR1* probes.

High-resolution micrococcal nuclease mapping

Preparation of nuclei was carried out as described previously (21,22). Briefly, nuclei were isolated from yeast cells, which were grown to mid-log phase (OD_{600} = 1). The nuclear pellet from a 1 liter culture was resuspended in 2.4 ml digestion buffer (10 mM HEPES, pH 7.5, 0.5 mM $MgCl_2$ and 0.05 mM $CaCl_2$). The suspension was divided into 400 μl portions, each of which was digested at 37°C for 10 min by using increasing concentrations (0–16 U/ml) of micrococcal nuclease (MNase; Amersham Biosciences). The reaction was terminated by adding EDTA, and the DNA was purified after treatment with RNase, proteinase K digestion and phenol–chloroform extraction. The purified DNA was resuspended in 0.1× TE (1 mM Tris–HCl, pH 8.0, 0.1 mM EDTA). MNase cleavage sites were detected by multiple rounds of *Taq* DNA polymerase-based primer extension. The primer (5′-TATGTCTAGTATGCTGGATTTAAACTCAT-3′) was end-labeled by T4 polynucleotide kinase. The cycling program was 94°C for 1 min, 53°C for 2 min and 72°C for 2 min for 35 cycles, and was followed by a 10 min chase at 72°C. The products were electrophoresed on a 6% polyacrylamide–8 M urea gel. The gel was dried and used to expose X-ray film. Relative MNase sensitivity was expressed graphically after scanning the autoradiogram and analyzing the scan by the NIH Image program (version 1.62).

Chromatin immunoprecipitation assay

The chromatin immunoprecipitation (ChIP) assay was performed essentially as described previously (23,24). A 50 ml culture of yeast (OD_{600} = 1) was treated with formaldehyde (final concentration of 1%) for 30 min at 20°C, and 2.5 ml of 2 M glycine was added to stop the cross-linking reaction. Cells were harvested and disrupted by vortexing in the presence of glass beads, and the lysate was sonicated to generate DNA fragments that ranged in size from 200 to 800 bp. To immunoprecipitate Myc-tagged proteins and Sir2p, we incubated anti-Myc antibody (9E10, Roche, Indianapolis, IN) and anti-Sir2p antibody (Santa Cruz Biotech., Santa Cruz, CA), respectively, with the extract overnight at 4°C, and the extract–antibody mixture then was incubated for an additional 3–4 h with protein G Sepharose beads (Amersham Biosciences). In some experiments, Myc-blocking peptide (Roche, final concentration 313 μg/ml) was added. Immunoprecipitates were washed with 1 ml each of lysis buffer (50 mM HEPES, pH 7.5, 140 mM NaCl, 1 mM EDTA, 1% Triton X-100, 0.1% sodium deoxycholate, 1 mM phenylmethylsulfonyl fluoride, 1 μg/ml leupeptin and 1 μg/ml pepstatin A), lysis buffer supplemented with 250 mM NaCl (for Myc-tagged Sas proteins) or 500 mM

NaCl (for Sir2p), LiCl–detergent wash buffer (250 mM LiCl, 10 mM Tris–HCl, pH 8.0, 1 mM EDTA, 0.5% NP-40 and 0.5% sodium deoxycholate) and TE. DNA was eluted with elution buffer (50 mM Tris–HCl, pH 8.0, 10 mM EDTA and 1% SDS). After reversal of the formaldehyde-induced cross-links, 1/5000 of input DNA and 1/45 of each immunoprecipitated DNA were used as templates for amplification by PCR. The sequences of primers for PCR were as follows: for the *HMLα* region, 5′-ATGCTCAGCTAGACGTTTTTCTTTC-3′ and 5′-TATGTCTAGTATGCTGGATTTAAACTCAT-3′; for the *ACT1* promoter region, 5′-CTTTTTCTTCCACGTCCTCTT-GC-3′ and 5′-TGGGATGGTGCAAGCGC-3′; and for the sub-telomeric chromatin at 7.5 kb from the end of chromosome VI, 5′-TCATGGTCTTGACAACTTTATGCG-3′ and 5′-TATC-TGACGTGAAAGTTCAGCGC-3′. Amplification was performed in a 20 µl reaction volume. The number of PCR cycles yielding product within the linear range was determined by analysis of 2-fold serial dilutions of the starting materials, and PCR products were separated on a 6% polyacrylamide gel and were detected by autoradiography. For quantitative analysis, 0.025 µl of [^{32}P]dCTP (110 TBq/mmol; Amersham Biosciences) was added to the PCR. After electrophoresis, the gel was dried, and the radioactivity corresponding to a specific band was measured by a bioimage analyzer (model BAS 1800II, Fuji Film, Tokyo, Japan).

Determination of the molecular size of the SAS-containing complex

Whole-cell extracts were prepared as described previously (11,25). Approximately 0.4 mg of each whole-cell extract was loaded onto a 2.4 ml Superdex 200 PC 3.2/30 column (Amersham Biosciences) that had been equilibrated in buffer containing 50 mM Tris–HCl, pH 8.0, 500 mM NaCl, 10% glycerol, 0.1% Tween-20, 1 mM phenylmethylsulfonyl fluoride, 0.5 µg/ml leupeptin and 0.5 µg/ml pepstatin A. A 10 µl aliquot of each fraction was electrophoresed in an SDS–polyacrylamide gel, transferred to nitrocellulose membrane and detected with the ECL western blotting analysis detection system (Amersham Biosciences). Anti-Myc antibody (9E10, Roche) was used.

RESULTS

HMLα2 was derepressed in a *sas2 sir1*-deleted strain

The α2 protein, which is a repressor of transcription of a-specific genes, is encoded by *MATα* and an essential factor for the regulation of mating-type-specific genes in α cells (26). The silent α information is also stored at the *HMLα* locus in both **a** and α cells. Previous work showed that the deletion of either *SIR1* or *SAS2* results in a very slight reduction of mating activity in a *MAT***a** strain, as indicated by quantitative mating analysis. The combined deletion of *SIR1* and *SAS2* strain causes a much more severe mating defect than that of the wild-type strain or the single-deletion strains (10,11). To show that the double deletion of *SAS2* and *SIR1* directly affects silencing at *HMLα*, we performed northern blotting analysis to detect the level of α2 mRNA in wild-type and deletion strains. α2 was transcribed not only in *MATα* cells but also in *sir4Δ* and *sas2Δsir1Δ MAT***a** cells (Figure 1A).

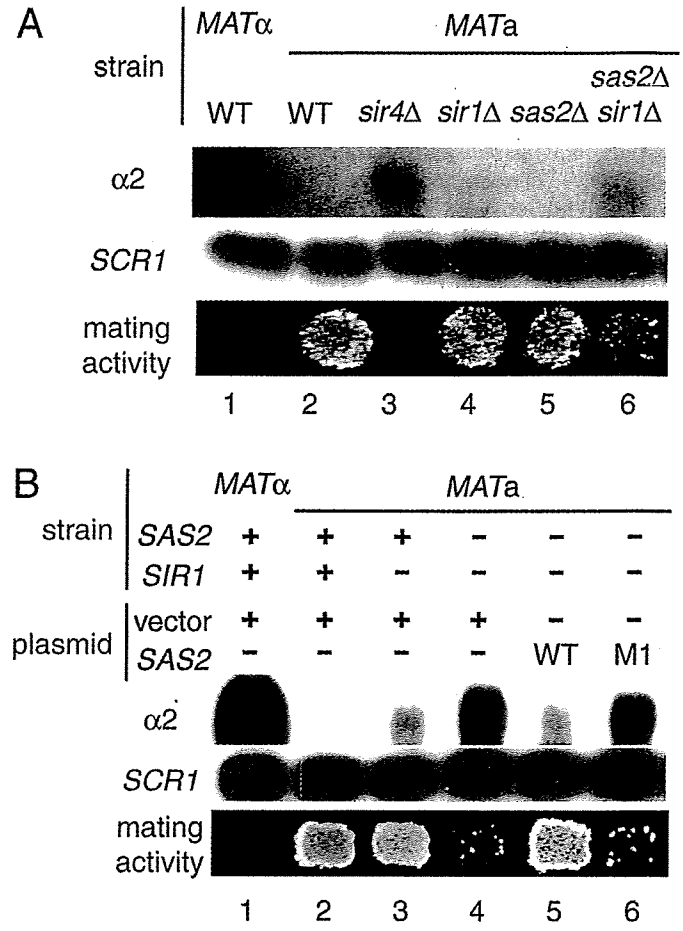

Figure 1. Deletion of *SAS2* and *SIR1* in a *MAT***a** strain leads to derepression of *HMLα2* expression and a non-mating. (**A**) RNA from either wild-type (WT, W303-1b and W303-1a), *sir4Δ* (YJW257), *sir1Δ* (YJW252), *sas2Δ* (YJW253) or *sas2Δsir1Δ* (YJW258) strains was hybridized by northern blotting to a probe specific for either the α2 or *SCR1* gene. RNA loading was standardized to *SCR1*. A qualitative mating assay was performed by patches, which were replica-plated to a lawn of *MATα* cells. WT and mutant strains are presented at the top of the panel. (**B**) A *sas2sir1* double-deletion strain was transformed with a plasmid carrying the WT or a mutant form of the *SAS2* gene (M1) under the control of its own promoter. Strains analyzed (ordered from left to right) were YSM119, YSM118, YSM120, YSM121, YSM122 and YSM123.

We previously showed that wild-type *SAS2*, but not *SAS2* with a mutation in the conserved HAT domain, could restore the mating activity of the *sas2Δsir1Δ* strain. Furthermore, this mutation of amino acids 219–221 (GLG) to alanine residues (termed *SAS2*-M1) abolished the HAT activity of Sas2p but did not affect the formation of the SAS complex (11,13). To determine whether Sas2p HAT activity is required for the repression of α2 expression, wild-type and mutant *SAS2* alleles were transformed into the *sas2Δsir1Δ* strain (Figure 1B). The mating activity and RNA level of α2 in the *sir1* mutant were the same as those of the *sas2 sir1* double-deletion strain carrying the wild-type *SAS2* expression plasmid (Figure 1B, compare lanes 3 and 5). *SAS2*-M1 failed to restore mating activity and α2 repression to the *sas2 sir1* double-mutant strain (Figure 1B, compare lanes 4 and 6). These results suggest that the Sas2p HAT activity is required for the repression of α2 expression from *HMLα* in a *sir1* mutant.

A strain with deletions of *SIR1* and *SAS2* shows loss of nucleosome organization at *HMLα*

The unique and highly organized chromatin structure of *HMLα* has been determined by high-resolution chromatin mapping analysis using MNase, which preferentially cuts the linker DNA between nucleosomes (27). Although a precisely positioned nucleosome (NUCα2) covers the transcription start site of the α2 gene at the *HMLα* locus, the promoter region of the α2 gene is nucleosome-free [(27); see also Figure 2A lanes 6–8 and Figure 2B]. We used MNase mapping to examine the effect of *sas2* mutations on the chromatin structure of *HMLα*. Deletion of *SIR4*, which is essential for *HMLα* silencing, resulted in increased nuclease sensitivity of one site, indicated by the arrow, compared with that of the wild type (Figure 2A, compare lanes 6–8 with lanes 10–12). Although we used downstream and reverse-strand primers in the attempt to visualize the positioning of NUCα2 clearly, we failed to obtain sufficient quantities of primer-extension products. For easy comparison of the MNase sensitivity, the lane treated with the highest concentration of MNase was selected for scanning (Figure 2A, lanes 8, 12, 16, 20 and 24). Relative MNase sensitivity is shown in Figure 2B after scanning and analyzing with the NIH Image software. The intensity of the induced sensitivity of the site highlighted in Figure 2A is the same in *sas2 sir1* double-deleted cells as in *SIR4*-deleted cells (compare lanes 10–12 with lanes 22–24) and stronger than that of wild-type or singly deleted strains (compare lanes 6–8, 14–16 and 18–20 with lanes 22–24). The MNase sensitivity of this site in different mutants correlates inversely with their mating activity and directly with the level of α2 mRNA (Figure 1A). These results suggest that *SAS2* is essential for the organization of the nucleosome precisely positioned over the transcriptional initiation site of the α2 in a *sir1*-mutant strain.

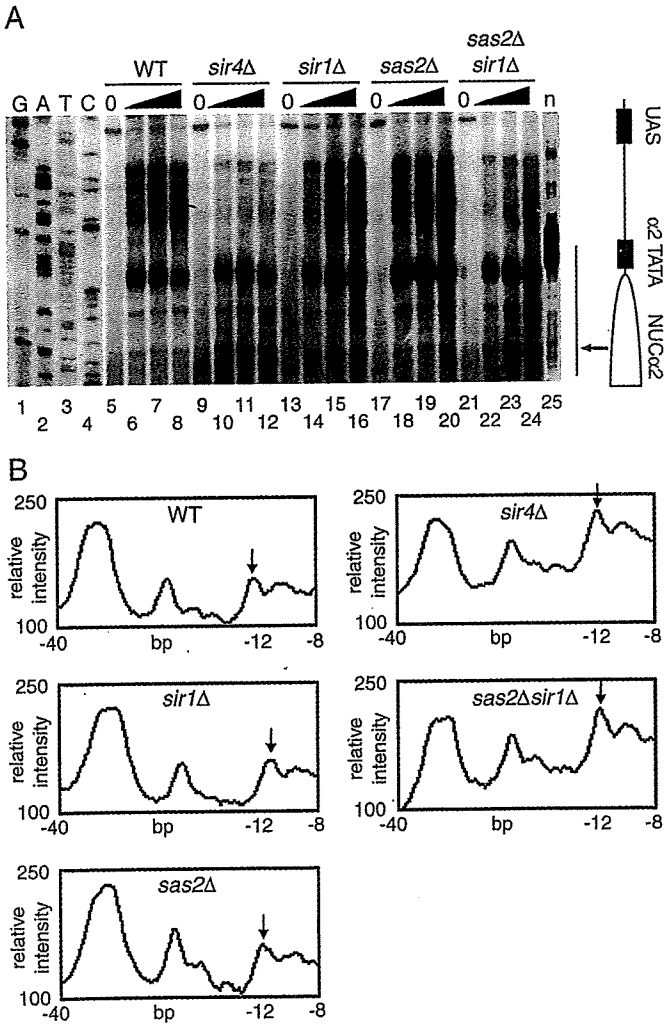

Figure 2. High-resolution MNase mapping of the promoter region of the α2 gene at the *HMLα* locus. (**A**) The chromatin structure of the Crick strand was mapped by primer-extension analysis of MNase-digested sites with the primer located at the coding region of the α2 gene. Strains used were as in Figure 1A. Extensions of undigested (0) and dose-dependent-digested chromatin are indicated. The 'n' lane shows the naked DNA digested with MNase (lane 25). The G, A, T and C columns indicate dideoxynucleotide-terminated sequencing reactions (lanes 1–4). The ellipse corresponds to the inferred position of the nucleosome, and boxes show the positions of the TATA-box and UAS regions. Arrow indicates sites in the α2 gene whose nuclease-sensitivity was increased in mutants relative to WT. The vertical bar indicates the region used for scanning to express the relative intensity in Figure 2B. (**B**) The relative MNase sensitivity expressed graphically after scanning and analyzing the autoradiogram in (**A**) by using NIH Image 1.62 software. Increased levels of nuclease-sensitive sites of the α2 gene in mutants (*sir4Δ* and *sas2Δsir1Δ*) relative to WT are indicated by arrows. The position from the transcription start site is shown at the bottom of each panel.

Interestingly, the nuclease sensitivity of the region between the UAS and TATA-box regions was decreased in *sas2Δsir1Δ* and *sir4Δ* strains. This region is generally less nuclease sensitive at *MATα* than at *HMLα* (27), and it is thought that in α2-positive cells, the protection of this region in chromatin from the nuclease might result from an association of transcription factors, including Rap1p, which bind to UAS (27). Overall, chromatin in this region is less accessible to nuclease in *sas2Δsir1Δ* strain than in wild-type strains.

The SAS complex associates with the *HMLα* locus

Genetic experiments revealed that combining the null allele of *SIR1* with that of *SAS2*, *SAS4*, *SAS5* or *ASF1* results in the reduction of silencing at *HMLα* (11,17). Meijsing and Ehrenhofer-Murray (12) reported that Sas2p is physically present at the rDNA locus, but not *ACT1*. To determine whether Sas2p or the SAS complex is located at the *HMLα* locus, we performed ChIP analysis using strains expressing Sas2p–Myc. Immunoprecipitated DNA was amplified by PCR with a primer pair spanning the α1 and α2 promoter regions in the *HMLα* locus (Figure 3A). We used *ACT1*, a gene whose transcription is not regulated by *SAS2*, as a negative control, because the *ACT1* mRNA level in the *sas2* mutant was same as that in the wild-type strain (15). Two-fold serial dilutions of the input and the immunoprecipitated DNA were performed to verify that the amount of PCR product was dependent on the starting material. Input DNA also was used as a template to confirm that these regions were amplified equally by PCR. In a *SAS2–Myc* strain, Sas2p–Myc associated with the promoter regions of the α1 and α2 in the *HMLα* region relative to *ACT1* (Figure 3A). This association was completely competed by adding a Myc-blocking peptide (compare lanes 11 and 12 with lanes 13 and 14).

We previously purified a complex containing Sas2p and showed that Sas4p and Sas5p were components of this

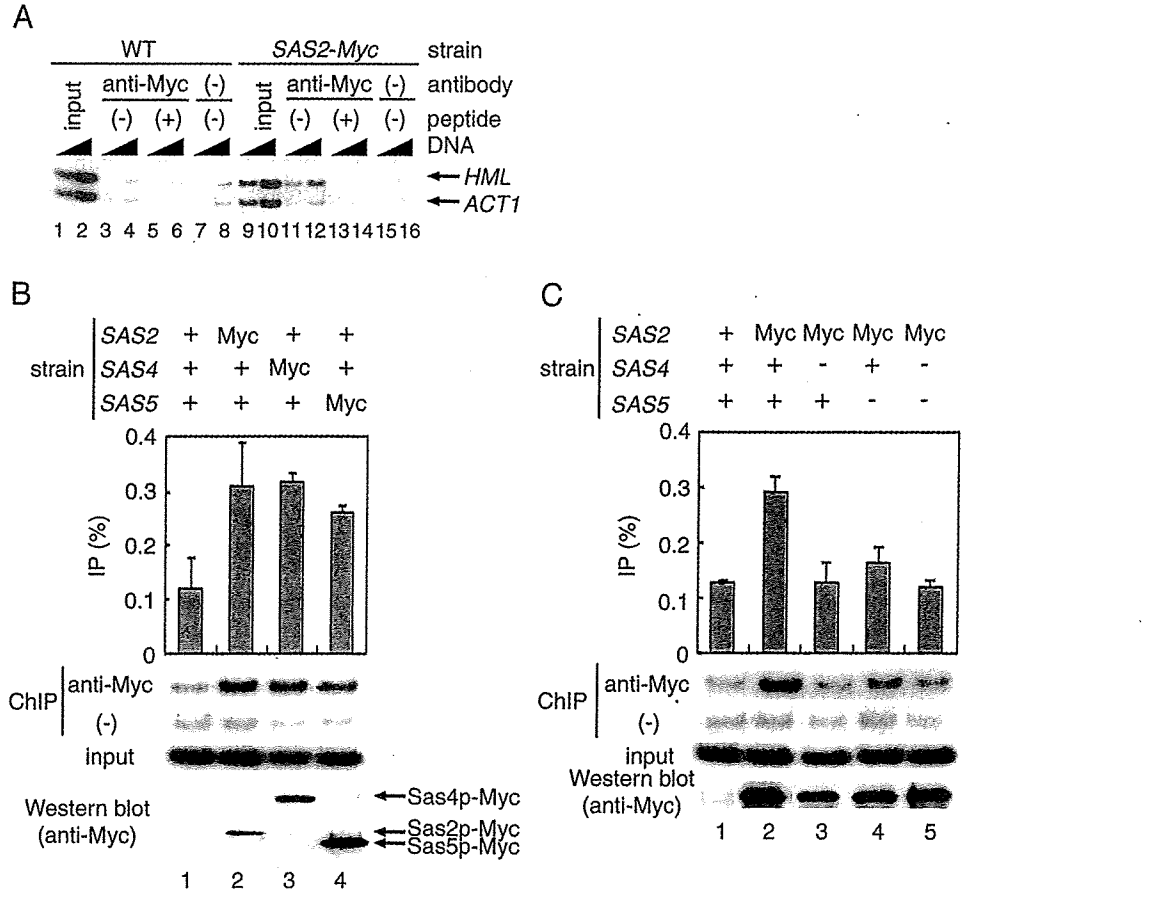

Figure 3. The SAS complex occupancy at the promoter in the *HMLα* locus. (**A**) Association of Sas2p with the *HMLα* region is detected by the ChIP assay. Sonicated chromatin was prepared from wild-type (WT) and Sas2p–Myc-expressing (YJW265) strains. Immunoprecipitation was carried out using monoclonal antibodies to the Myc tag (lanes 3–6 and 11–14), and normal IgG was used as a negative control (lanes 7, 8, 15 and 16). Myc-blocking peptide was added in some immunoprecipitation experiments (lanes 5, 6, 13 and 14). Input and immunoprecipitated DNA were amplified by PCR using primer pairs spanning the promoter region of α1 and α2 genes or *ACT1*. PCR products were resolved on a 6% polyacrylamide gel and visualized by autoradiography. (**B**) Localization of subunits of the SAS complex to the promoter of the α1 and α2 genes. Soluble chromatin was prepared from the strains that expressed the C-terminal Myc epitope-tagged Sas2p (YJW265), Sas4p (YJW228) or Sas5p (YJW229), and immunoprecipitated with or without anti-Myc antibody. Final DNA extractions were amplified with [^{32}P]dCTP. The PCR product was separated on the polyacrylamide gel and quantitated with a bioimage analyzer after drying the gel. ChIP efficiency is reported as a percentage of immunoprecipitated material (top panel). Data are presented as the mean ± SD from three independent experiments. Input DNA (input) was equally amplified by PCR in WT and Sas2p–Myc-expressing strains. Myc-tagged proteins were detected by western blotting (bottom panel). (**C**) *SAS4* or *SAS5* or both are required for the recruitment Sas2p to the *HMLα* locus. ChIP assay was performed with chromatin prepared from *sas4Δ* (YJW269), *sas5Δ* (YJW270) and *sas4Δsas5Δ* (YJW271) strains that expressed the C-terminal Myc epitope-tagged Sas2p. Results are shown as in Figure 3B.

complex, termed the SAS complex (11,13,14). We next asked whether Sas4p and Sas5p associate with the *HMLα* locus. ChIP analyses using *SAS4–Myc* and *SAS5–Myc* revealed that Sas4p–Myc and Sas5p–Myc were recruited together with Sas2p–Myc to the promoter regions of the α1 and α2 in the *HMLα* region (Figure 3B). This finding supports the possibility that these Sas proteins associate with chromatin as a complex. Accordingly, deletion of either *SAS4* or *SAS5* might disrupt the association of Sas2p with the *HMLα* locus.

To evaluate whether this disruption occurs, we performed ChIP using cells expressing Sas2p–Myc and deleted for *SAS4*, *SAS5* or both genes (Figure 3C). The amount of amplified PCR products from the three deletion strains was markedly lower than from the wild-type strain, although Sas2p–Myc was expressed efficiently in all of the *SAS2–Myc* strains. These results show that mutations in *SAS5* and especially *SAS4* inhibit the association of Sas2p–Myc with the promoter regions of the α1 and α2 in the *HMLα* region and that Sas2p–Myc was recruited to this region as a component of the SAS complex.

SIR1 and *SIR2* are not required for the recruitment of Sas2p to the promoters in the *HMLα* locus

Four Sir proteins localize to *HMLα* and *HMR***a** and are important for silencing. Sir1p binds to Orc1p, one of the silencer binding proteins, and helps to recruit Sir4p. Sir2p, Sir3p and Sir4p form a complex and spread in both directions from the silencers (1,28). A physical interaction between Sas and Sir proteins has not been reported, although all of them localize to the *HMLα* locus. To understand the role of the Sir proteins in the association of Sas2p with the *HMLα* locus, we first asked whether loss of Sir1p or Sir2p results in disruption of this association. To do this, Sas2p was tagged with Myc in *SIR1* or *SIR2* deletion strains. Western blot analysis revealed that Sas2p–Myc was expressed efficiently in both *SIR1* and *SIR2*

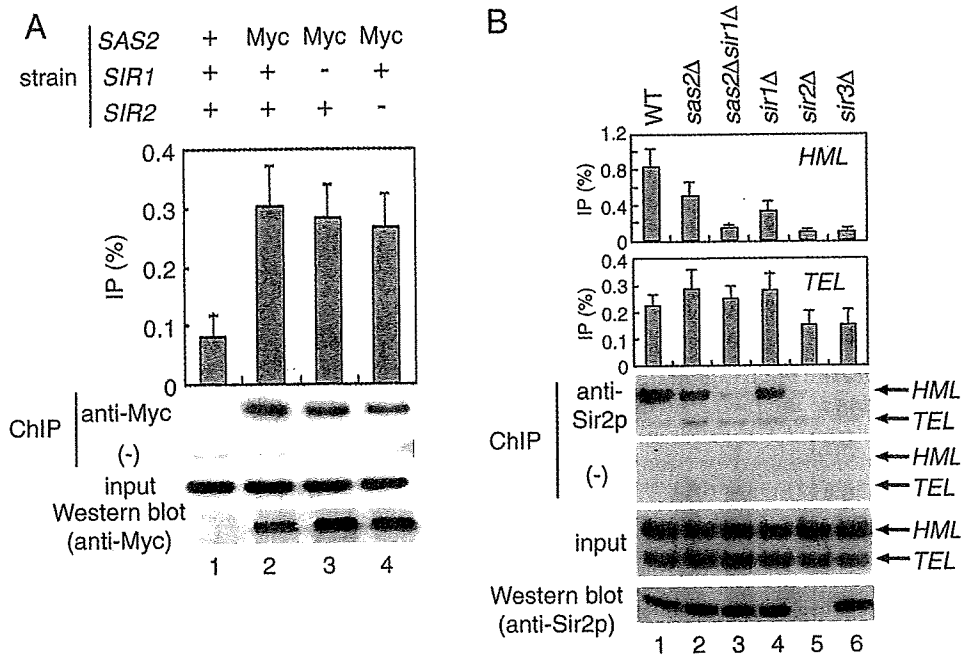

Figure 4. (**A**) *SIR1* and *SIR2* are not required for the recruitment of Sas2p to the promoter in the *HMLα* locus. ChIP assay was performed with chromatin prepared from *sir1*Δ (YSM85) and *sir2*Δ (YSM90) strains that expressed the C-terminal Myc epitope-tagged Sas2p. (**B**) Effect of deletion of *SAS2* and *SIR* genes on the Sir2p occupancy. Soluble chromatin was prepared from wild-type and deletion strains, and immunoprecipitated with or without anti-Sir2p antibody. Strains analyzed (ordered from left to right) were W303-1a, *sas2*Δ (YJW253), *sas2*Δ*sir1*Δ (YJW258), *sir1*Δ (YJW252), *sir2*Δ (YSM64) and *sir3*Δ (YS480). Results are shown as in Figure 3B.

deletion strains (Figure 4A). We prepared chromatin fractions from these strains and subjected them to ChIP analysis for the Myc epitope. As shown previously, Sas2p–Myc associated with the *HMLα* region in wild-type cells. Loss of *SIR1* or *SIR2* did not affect this association (Figure 4A). This finding indicates that *SIR1* and *SIR2* are not required for the recruitment of Sas2p to the promoters in the *HMLα* locus.

Disruption of *SAS2* in a wild-type strain increased the spreading of Sir proteins to the sub-telomeric region (15,16). Deletion of *SAS2* in a *sir1* mutant also may lead to spreading of the finite number of Sir2p molecules into sub-telomeric regions, resulting in a decrease in Sir2p occupancy at the *HMLα* locus. To test this hypothesis, we asked whether loss of *SAS2* results in increased or decreased Sir2p association. We observed localization of Sir2p in the regions of the *HMLα* locus and sub-telomeric chromatin 7.5 kb from the end of chromosome VI in the wild-type and deletion strains (Figure 4B). Consistent with previous observations, the Sir2p association detected within the *HMLα* locus and sub-telomeric regions in the wild-type strain was greater than that in a *sir2* deletion strain (Figure 4B, compare lanes 1 and 5) and was slightly increased in the sub-telomeric region by *SAS2* deletion (16,29). Interestingly, although Sir2p was expressed efficiently in all of the strains except a *sir2* deletion strain, the disruption of *SAS2* or *SIR1* decreased the amount of Sir2p localization at the *HMLα* locus (Figure 4B). In the combination of *SAS2* deletion with the null allele of *SIR1*, the Sir2p association at the *HMLα* locus was completely lost, similar to that in the *SIR2* and *SIR3* deletion strains. This indicates that although Sas2p association at the *HMLα* locus does not require *SIR1* or *SIR2*, Sir2p localization is partially dependent on *SAS2*.

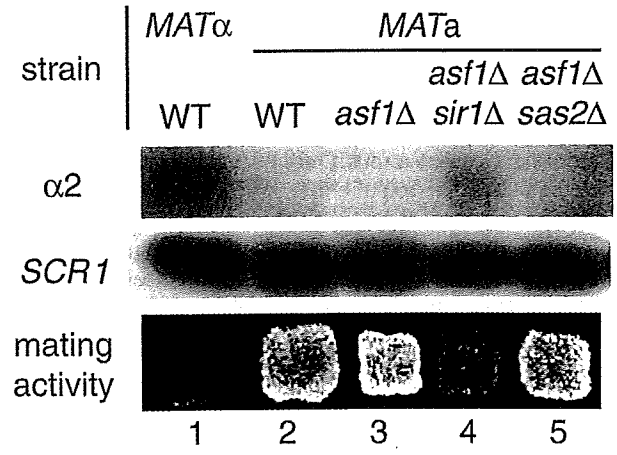

Figure 5. *ASF1* and *SAS2* function in the same pathway in *HMLα* silencing. Disruption of *ASF1* in combination with a null allele of *SIR1*, but not of *SAS2*, derepressed α2 expression. RNA from either wild-type (WT: W303-1b and W303-1a), *asf1*Δ (YJW433), *asf1*Δ*sir1*Δ (YJW435) or *asf1*Δ*sas2*Δ (YJW436) was hybridized by northern blotting to a probe specific for either the α2 or *SCR1* gene. A qualitative mating assay was performed by patches, which were replica-plated to a lawn of α cells.

α2 expression in the *asf1 sir1* deletion strain

We and others (11,12) previously showed that the SAS complex physically interacts with Asf1p and these factors function in a pathway that enhances the epigenetic silencing defects of *sir1* mutants. To learn more about the function of *ASF1* in the *HMLα* silencing, we measured the expression of α2 in an *ASF1* deletion strain (Figure 5). Deletion of *ASF1* results in a very slight reduction in silencing at *HMLα* as indicated by

quantitative mating analysis (11), and the α2 mRNA level in the *asf1* mutant was indistinguishable from that of the wild-type strain. We previously showed that the combined deletion of *ASF1* and *SIR1* caused much more severe silencing defects at *HMLα* than does the deletion of *ASF1* alone (11). Derepression of α2 repression occurred in the *asf1 sir1* double-deletion strain but not in the *asf1Δsas2Δ* strain. Loss of mating activity correlated with the increased α2 expression in the *asf1 sir1* deletion strain (Figure 5).

Loss of *ASF1* disrupts the recruitment of the SAS complex to the *HMLα* locus

We showed that *SIR1* and *SIR2* are not required for the recruitment of Sas2p to the promoters in the *HMLα* locus (Figure 4). Next, we investigated whether *ASF1* is required for Sas2p–Myc recruitment. Loss of *ASF1* markedly decreased Sas2p association with the *HMLα* locus (Figure 6A). This decrease was restored by a plasmid carrying *ASF1* (compare lanes 3 and 4). In a *sir1* mutant, the effect of *ASF1* on the Sas2p recruitment was the same as for the *SIR1* wild-type strain. These results indicate that *ASF1*, but not *SIR1*, is required for the recruitment of Sas2p to the *HMLα* locus. Sas2p expression levels in whole-cell extracts from wild-type, *asf1Δ*, and *asf1Δsir1Δ* strains were indistinguishable, and disruption of *ASF1* did not affect the size of the SAS complex (Figure 6A and B). These data indicate that loss of the association of Sas2p with the *HMLα* locus in the *asf1* mutants is not due to a decrease in Sas2p expression or disruption of the SAS complex.

DISCUSSION

Deletion of *SIR1* in combination with a null allele of either *SAS2* or *ASF1* causes a much more severe silencing defect at *HMLα* than does deletion of either gene alone (11), but the role of these factors in silencing was unclear. We showed that the combination of mutation of *SAS2* with *SIR1* induced derepression of α2 expression and changed the precisely positioned nucleosome that includes the transcriptional initiation site of the α2, and that the HAT activity of Sas2p is critical for this effect. Furthermore, ChIP assays revealed specific association of the SAS complex with the *HMLα* locus, and the SAS complex recruitment required *ASF1* but not *SIR1* and *SIR2*.

The effect of the disruption of *SAS2* on silencing is different among loci. For example, normal *HMR***a** silencing is unaffected by *SAS2* deletion, but *sas2* mutations suppress the silencing defect caused by mutation in the silencer elements of *HMR***a** (10,17). Deletion of *SAS2* leads to loss of hyperacetylation of histone H4 at lysine 16 in regions adjacent to telomeres. This results in the spreading of Sir3p away from the telomeres into these sub-telomeric regions, leading to repression of gene expression in the sub-telomeric region (15,16). However, deletion of *SAS2* causes the loss of silencing at the telomeres themselves, presumably because of titration of Sir proteins away from this locus.

In present study, Sas2p was found to be associated with the *HMLα* locus, and Sir2p was not required for this Sas2p association. Disruption of *SAS2* increased the spreading of Sir proteins to the sub-telomeric region (15,16). Deletion of *SAS2* in *sir1* mutants also led to the spreading of the finite number of

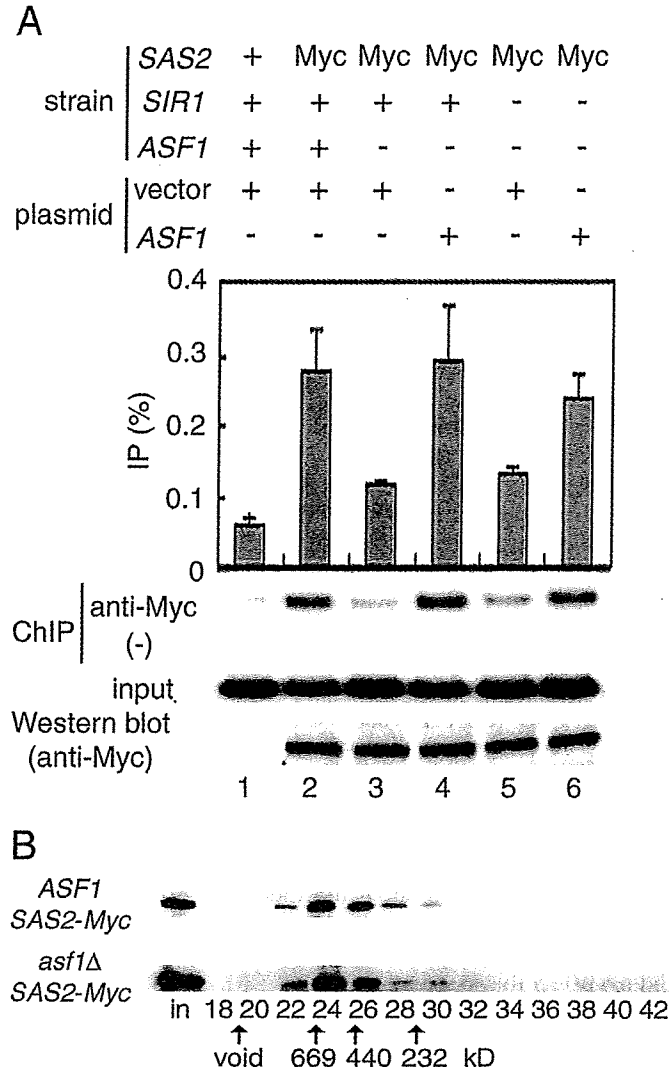

Figure 6. Sas2 occupancy at the *HMLα* region is dependent on *ASF1*. (**A**) Chromatin was prepared from the Sas2p–Myc-expressing strains containing either an empty vector or a CEN-based *ASF1* plasmid expressed from its own promoter. Strains for the ChIP assay (ordered from left to right) were YSM112, YSM113, YSM114, YSM115, YSM116 and YSM117. Results are shown as in Figure 3B. (**B**) Comparison of the Sas2p–Myc elution profiles from Superdex 200 size exclusion chromatography after fractionation of whole-cell extracts prepared from wild-type (YJW265) and *asf1Δ* (YSM87) mutant strains. Shown are western blots of column fractions probed with the anti-Myc antibody.

Sir2p molecules into sub-telomeric regions and resulted in a decrease in Sir2p occupancy at the *HMLα* locus. We also showed that the Sas2p HAT activity is essential for α2 repression. Acetylation of lysine 16 of histone H4 might be a landmark for Sir2p assembly: once lysine 16 of histone H4 is acetylated by Sas2p, Sir2p recognizes and deacetylates that residue in the silenced domain and is held in this region. Sas2p might contribute to regulating the histone H4 lysine 16 acetylation state at the chromosome level as well as at the locus level. Deletion of *ASF1* likely would bring about the same phenomenon, because we found that Sas2p occupancy at the *HMLα* locus was dependent on *ASF1*. Other investigators have shown that the association of Sir proteins at the *HMLα* silencer is somewhat reduced in *sir1*-mutant cells (29). The deletion of

SIR1 in combination with null alleles of either *SAS2* or *ASF1* may decrease the association of Sir proteins to a much greater extent than that seen after deletion of *SIR1* only, thereby causing a much more severe silencing defect at *HMLα* than that seen after deletion of either gene alone.

We previously showed that Sas4p, one of the subunits of the SAS complex, directly interacts with Asf1p (11). Therefore, recruitment of the SAS complex to the *HMLα* region might require physical interaction with Asf1p. In the present study, we found that the SAS complex is associated with the *HMLα* region, but not the *ACT1* promoter. However, Moshkin *et al.* (30) showed that *Drosophila* Asf1 associated with multiple sites, including heterochromatic and transcriptionally active regions. Furthermore, *asf1* mutants are defective in the repression of histone gene transcription during the cell cycle and in cells arrested in the early S phase (31). Finally, Asf1 interacts with bromodomain-containing subunits of TFIID and the Brahma complex, a member of the SWI/SNF ATP-utilizing chromatin-remodeling factors (30,32). These results indicate that *ASF1* affects transcriptional control through a variety of mechanisms. The estimated numbers of Asf1p and Sas4p molecules per yeast cell are 6230 and 768, respectively (33). This distribution suggests that the SAS complex interacts with a subset of Asf1 proteins. The mechanism of the recruitment specificity of the SAS complex is still unknown. *HMLα* binding factors other than Sir proteins may enhance the SAS complex association with the *HMLα* locus. Alternatively, Asf1p-associated factors that selectively bind to Asf1p within transcriptionally active regions may inhibit the interaction between the SAS complex and Asf1p. To address this possibility, we are purifying the factors that interact with the SAS complex and Asf1p.

ACKNOWLEDGEMENTS

The authors gratefully acknowledge Drs Xi Wang and Robert Simpson (Pennsylvania State University) for assistance in establishing the chromatin mapping methods in our laboratory. The authors thank Drs Jerry Workman, Ann Sutton, Rolf Sternglanz, David Rivier and Peter Philippsen for kindly providing yeast strains and plasmids. The authors also thank Drs Ann Sutton, LeAnn Howe and Jerry Workman for critical reading of the manuscript and for advice in designing experiments. The authors thank the staff of the Radioisotope Research Center, Osaka University, and the Central Laboratory for Research and Education, Osaka University Medical School. This research was supported in part by grants from the Japanese Ministry of Education, Culture, Sports, Science and Technology (MEXT), the NISSAN Science Foundation, the Inamori Foundation and the Sasakawa Scientific Research Grant from the Japan Science Society. Funding to pay the Open Access publication charges for this article was provided by MEXT.

Conflict of interest statement. None declared.

REFERENCES

1. Lustig,A.J. (1998) Mechanisms of silencing in *Saccharomyces cerevisiae*. *Curr. Opin. Genet. Dev.*, **8**, 233–239.
2. Huang,Y. (2002) Transcriptional silencing in *Saccharomyces cerevisiae* and *Schizosaccharomyces pombe*. *Nucleic Acids Res.*, **30**, 1465–1482.
3. Sterner,D.E. and Berger,S.L. (2000) Acetylation of histones and transcription-related factors. *Microbiol. Mol. Biol. Rev.*, **64**, 435–459.
4. Carrozza,M.J., Utley,R.T., Workman,J.L. and Cote,J. (2003) The diverse functions of histone acetyltransferase complexes. *Trends Genet.*, **19**, 321–329.
5. Richards,E.J. and Elgin,S.C. (2002) Epigenetic codes for heterochromatin formation and silencing: rounding up the usual suspects. *Cell*, **108**, 489–500.
6. Cockell,M., Gotta,M., Palladino,F., Martin,S.G. and Gasser,S.M. (1998) Targeting Sir proteins to sites of action: a general mechanism for regulated repression. *Cold Spring Harbor Symp. Quant. Biol.*, **63**, 401–412.
7. Tanny,J.C., Dowd,G.J., Huang,J., Hilz,H. and Moazed,D. (1999) An enzymatic activity in the yeast Sir2 protein that is essential for gene silencing. *Cell*, **99**, 735–745.
8. Imai,S., Armstrong,C.M., Kaeberlein,M. and Guarente,L. (2000) Transcriptional silencing and longevity protein Sir2 is an NAD-dependent histone deacetylase. *Nature*, **403**, 795–800.
9. Pillus,L. and Rine,J. (1989) Epigenetic inheritance of transcriptional states in *S. cerevisiae*. *Cell*, **59**, 637–647.
10. Reifsnyder,C., Lowell,J., Clarke,A. and Pillus,L. (1996) Yeast SAS silencing genes and human genes associated with AML and HIV-1 Tat interactions are homologous with acetyltransferases. *Nature Genet.*, **14**, 42–49.
11. Osada,S., Sutton,A., Muster,N., Brown,C.E., Yates,J.R.,III, Sternglanz,R. and Workman,J.L. (2001) The yeast SAS (something about silencing) protein complex contains a MYST-type putative acetyltransferase and functions with chromatin assembly factor ASF1. *Genes Dev.*, **15**, 3155–3168.
12. Meijsing,S.H. and Ehrenhofer-Murray,A.E. (2001) The silencing complex SAS-I links histone acetylation to the assembly of repressed chromatin by CAF-I and Asf1 in *Saccharomyces cerevisiae*. *Genes Dev.*, **15**, 3169–3182.
13. Sutton,A., Shia,W.J., Band,D., Kaufman,P.D., Osada,S., Workman,J.L. and Sternglanz,R. (2003) Sas4 and Sas5 are required for the histone acetyltransferase activity of Sas2 in the SAS complex. *J. Biol. Chem.*, **278**, 16887–16892.
14. Shia,W.J., Osada,S., Florens,L., Swanson,S.K., Washburn,M.P. and Workman,J.L. (2005) Characterization of the yeast trimeric-SAS acetyltransferase complex. *J. Biol. Chem.*, **280**, 11987–11994.
15. Kimura,A., Umehara,T. and Horikoshi,M. (2002) Chromosomal gradient of histone acetylation established by Sas2p and Sir2p functions as a shield against gene silencing. *Nature Genet.*, **32**, 370–377.
16. Suka,N., Luo,K. and Grunstein,M. (2002) Sir2p and Sas2p opposingly regulate acetylation of yeast histone H4 lysine16 and spreading of heterochromatin. *Nature Genet.*, **32**, 378–383.
17. Xu,E.Y., Kim,S. and Rivier,D.H. (1999) SAS4 and SAS5 are locus-specific regulators of silencing in *Saccharomyces cerevisiae*. *Genetics*, **153**, 25–33.
18. Guthrie,C. and Fink,G.R. (1991) *Guide to Yeast Genetics and Molecular Biology*. Academic Press, San Diego, CA.
19. Longtine,M.S., McKenzie,A.,III, Demarini,D.J., Shah,N.G., Wach,A., Brachat,A., Philippsen,P. and Pringle,J.R. (1998) Additional modules for versatile and economical PCR-based gene deletion and modification in *Saccharomyces cerevisiae*. *Yeast*, **14**, 953–961.
20. Sprague,G.F.,Jr (1991) Assay of yeast mating reaction. *Methods Enzymol.*, **194**, 77–93.
21. Weiss,K. and Simpson,R.T. (1997) Cell type-specific chromatin organization of the region that governs directionality of yeast mating type switching. *EMBO J.*, **16**, 4352–4360.
22. Li,B. and Reese,J.C. (2001) Ssn6-Tup1 regulates RNR3 by positioning nucleosomes and affecting the chromatin structure at the upstream repression sequence. *J. Biol. Chem.*, **276**, 33788–33797.
23. Kuo,M.H. and Allis,C.D. (1999) *In vivo* cross-linking and immunoprecipitation for studying dynamic protein: DNA associations in a chromatin environment. *Methods*, **19**, 425–433.
24. Ausubel,F.M., Brent,R., Kingstone,R.E., Moore,D.D., Seidman,J.G. and Smith,J.A. (1999) *Current Protocols in Molecular Biology*. John Wiley & Sons, Inc., NY.
25. Eberharter,A., John,S., Grant,P.A., Utley,R.T. and Workman,J.L. (1998) Identification and analysis of yeast nucleosomal histone acetyltransferase complexes. *Methods*, **15**, 315–321.
26. Herskowitz,I., Rine,J. and Strathern,J. (1992) *The Molecular and Cellular Biology of the Yeast Saccharomyces*. Cold Spring Harbor Laboratory Press, Cold Spring Harbor, NY.

27. Weiss,K. and Simpson,R.T. (1998) High-resolution structural analysis of chromatin at specific loci: *Saccharomyces cerevisiae* silent mating type locus *HMLα*. *Mol. Cell. Biol.*, **18**, 5392–5403.
28. Triolo,T. and Sternglanz,R. (1996) Role of interactions between the origin recognition complex and SIR1 in transcriptional silencing. *Nature*, **381**, 251–253.
29. Rusche,L.N., Kirchmaier,A.L. and Rine,J. (2002) Ordered nucleation and spreading of silenced chromatin in *Saccharomyces cerevisiae*. *Mol. Biol. Cell*, **13**, 2207–2222.
30. Moshkin,Y.M., Armstrong,J.A., Maeda,R.K., Tamkun,J.W., Verrijzer,P., Kennison,J.A. and Karch,F. (2002) Histone chaperone ASF1 cooperates with the Brahma chromatin-remodelling machinery. *Genes Dev.*, **16**, 2621–2626.
31. Sutton,A., Bucaria,J., Osley,M.A. and Sternglanz,R. (2001) Yeast ASF1 protein is required for cell cycle regulation of histone gene transcription. *Genetics*, **158**, 587–596.
32. Chimura,T., Kuzuhara,T. and Horikoshi,M. (2002) Identification and characterization of CIA/ASF1 as an interactor of bromodomains associated with TFIID. *Proc. Natl Acad. Sci. USA*, **99**, 9334–9339.
33. Ghaemmaghami,S., Huh,W.K., Bower,K., Howson,R.W., Belle,A., Dephoure,N., O'Shea,E.K. and Weissman,J.S. (2003) Global analysis of protein expression in yeast. *Nature*, **425**, 737–741.